Imperial College London

MSc Quantum Fields and Fundamental Forces

# Reheating of the Universe and Gravitational Wave Production

*Author:*
Luisa Lucie-Smith

*Supervisor:*
Prof. Arttu Rajantie

*Submitted in partial fulfilment of the requirements*
*for the degree of Master of Science*
*of Imperial College London*

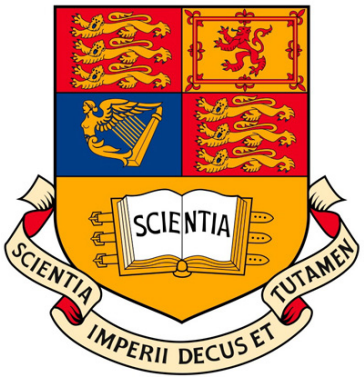


September 21, 2014

# Acknowledgements

First, I would like to thank my supervisor Prof. Arttu Rajantie for introducing me to this extremely interesting topic and for being so helpful and patient while carrying out this work with me. I also want to thank Dr. Laura Bethke for the useful discussions and for the help on the computational side of my work.

I would like to thank all the people on my course for all the technical and moral support I received, in particular Marc, Paul, James and Sonny. Most of all, I would like to thank Omar for always being next to me the last weeks and never giving up. You have been my greatest support. And thank you to Kalisha, for being my best friend.

I dedicate this thesis to my mother.

# Contents


**1 Introduction** **1**
- 1.1 Brief History of the Universe . . . 1
- 1.2 Inflation . . . 2
- 1.3 Reheating . . . 3
- 1.4 Gravitational Waves . . . 4
- 1.5 Outline of the thesis . . . 6

**2 Inflation** **7**
- 2.1 From the Hot Big Bang to Inflation . . . 7
- 2.2 Cosmological puzzles . . . 10
- 2.3 Slow-roll inflation . . . 13
- 2.4 Inhomogeneities from inflation . . . 17
  - 2.4.1 Quantum fluctuations . . . 19

**3 Reheating** **22**
- 3.1 Introduction: The two Stages of Reheating . . . 22
- 3.2 $\phi$ at the end of inflation . . . 23
- 3.3 Preheating . . . 25
- 3.4 Thermalization . . . 31
- 3.5 Non-minimal coupling to gravity . . . 31
  - 3.5.1 Values of $\xi$ . . . 33
  - 3.5.2 From the Jordan frame to the Einstein frame . . . 34
  - 3.5.3 Small $\xi$ approximation . . . 39
  - 3.5.4 Large $\phi$ approximation . . . 41
- 3.6 Numerical Simulations . . . 44
  - 3.6.1 Minimal coupling case . . . 47
  - 3.6.2 Non-minimal coupling case . . . 50

**4 Gravitational Waves** **55**
- 4.1 The Origin of Gravitational Waves . . . 55
- 4.2 Gravitational Waves Detectors . . . 56
- 4.3 Gravitational Waves from Reheating . . . 58
- 4.4 Numerical Simulations . . . 61
  - 4.4.1 Simulations on Gravitational Wave Production . . . 64

**5 Future Improvements** **67**

**6 Conclusions** **69**

# 1. Introduction

Cosmology is one of the most vast and fascinating areas of research in theoretical physics. It studies the origin, evolution and fate of the whole Universe. This thesis will focus on two aspects of the early Universe; the first part will discuss the epoch of reheating of the Universe and the second part will account for its phenomenological consequence of gravitational wave production. In this way, I will be able to provide both a theoretical understanding of the process of reheating and a prediction on observational signatures produced by it.

In this chapter, I will provide the necessary theoretical background and motivations for my research. I will briefly review the history of the Universe, the theory of inflation and the process of reheating in an introductory form. I will also define the nature of gravitational waves and discuss the importance of studying primordial gravitational waves produced during reheating.

## 1.1 Brief History of the Universe

In recent decades, physicists' understanding of the Universe has developed extraordinarily fast. The Universe was created around 13.7 billion years ago by a violent explosion known as the Big Bang. The hot Big Bang theory is the most successful theory to date describing the evolution of the Universe starting from $t \sim 10^{-33}$ seconds after the Big Bang [1].

At that time, the Universe was dense, hot, energetic and no particles yet existed. Gradually the Universe cooled down, entering the *radiation era* in which the radiation components of the Universe, principally photons and neutrinos, set the dynamics of the Universe. This era allowed for symmetry breaking to occur and the first particles to form. Most importantly, at around 100 seconds after the Big Bang, the Universe underwent the process of nucleosynthesis, where the first complex nuclei were formed [2]. Subsequent to the radiation era is the *matter era* in which the density of matter exceeds that of radiation at around $t \sim 100,000$ years after the Big Bang. This transition occurs since matter and radiation evolve differently as the Universe expands [3].

During the matter era, around $t \sim 380,000$ years after the Big Bang, photons decoupled and started free streaming at a time known as *recombi-*

*nation*. These photons are still present in the Universe today and create a quasi-isotropic radiation background which we call the Cosmic Microwave Background (CMB) (see figure 1.1.1) [4]. The CMB is of fundamental importance to cosmologists since it is a direct picture of the Universe during recombination. It was discovered accidentally by A. Penzias and R.W. Wilson in 1964 when they noticed a low and persistent noise while experimenting with a horn antenna built to detect radio waves [5]. The CMB carries direct information regarding the history of the Universe before and after the start of its radiation. Thanks to space-based observatories its features have been deeply studied, intially by COBE (Cosmic Background Explorer) in 1992 [6], WMAP (Wilkinson Microwave Anisotropy Probe) in 2003 [7] and PLANCK in 2012 [8]. In particular, over the past years these satellites have been mostly measuring the tiny fluctuations of the CMB.

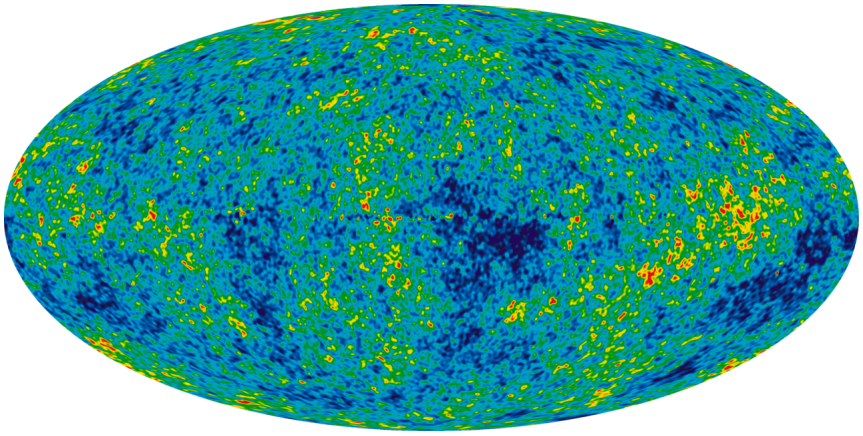

**Figure 1.1.1:** CMB fluctuations from 9 years of WMAP data showing a temperature of ± 200 microKelvin

Today, the Universe is dark-energy dominated and at a temperature of around 2.7 Kelvin, a state unchanged since $10^9$ years after the Big Bang.

## 1.2 Inflation

What is not as well understood yet is what happened in these fleeting moments following the Big Bang. The hot Big Bang theory is enormously successful with the CMB and for instance primordial nucleosynthesis. However, some facts remain unavoidably unexplained in the hot Big Bang model and the need of a larger framework seems necessary. In particular, why does the Universe result so homogenous? Why is it so close to flatness? And finally, why does the CMB result quasi homogenous and isotropic? The hot Big Bang model cannot explain these observational facts about the Universe.

The main theoretical model which was invented to account for these is that of an inflationary epoch [9]. Inflation consists of an extremely rapid

expansion of the Universe which occurred within $10^{-36}$ seconds after the Big Bang. The expansion occurred at exponential rate which blew apart the whole Universe. Inflation is the only model which has survived thirty years of cosmological data. The CMB fluctuations were created during inflation and can therefore provide essential information on the inflationary model driving the early Universe. However, many theories on the Universe's origin and evolution have been formulated and then tested by observations. Planck is a space-based observatory which measures fluctuations on the CMB and provides constraints on cosmological parameters and hence on the possible inflationary models. Many models have been ruled out, revised or improved based on Planck's data [10]. So far, there is still a broad range of inflationary models which predict today's data of the CMB. In the future, we hope to achieve more and more accuracy in the data in order to further restrict the number of possible inflationary theories.

In most modern inflationary models, all the energy of the Universe is carried by a scalar field, called the *inflaton* [11]. The effective potential of the system drives the evolution of the scalar field and hence the dynamics of inflation. The main constraint on the potential for inflation to occur in the first place is that it must be very flat. This allows the inflaton to live in a *slow-roll regime* during inflation, or in other words to slowly roll on the flat curve of the potential. It is this slow-roll regime which allows the Universe to expand exponentially [12]. Inflation ends once the inflaton reaches a steeper slope and it rolls down the slope to reach the minimum of the effective potential. Another necessary requirement is for inflation to last for a finite amount of time in order for the hot Big Bang model to preserve its success in the later stages[9]. Hence, inflation does not replace the hot Big Bang theory but it simply describes the Universe prior to when the Big Bang theory is valid.

## 1.3 Reheating

If the Universe went through an inflationary era, then Reheating must have followed it before the Universe enters the radiation era [11]. The inflationary model specifies the dynamics of inflation and it therefore also affects the phenomenology of the reheating process. Reheating sets the post-inflationary conditions of the Universe before it enters the radiation era. Once the Universe enters the radiation era, its evolution is described by the physics of the hot Big Bang model.

Essentially, all elementary particles are produced during reheating. This makes reheating one of the most fundamental phases predicted by inflationary models. However, the theory of reheating was the last part to be developed and understood of inflationary theory. Many different, and sometimes contradictory, papers were published to develop theories of reheating in different

inflationary scenarios. Two of the main reviews were published in 1997 by L.Kofman et.al. [13], [14] which cover in depth the main aspects of reheating and on which my review will mainly be based on.

The main idea is that reheating occurs once the slow-roll regime ends and the inflaton starts oscillating around the minimum of its effective potential. Recall that during inflation, all the energy is stored in one scalar field which we call inflaton. Elementary particles are produced by the inflaton's oscillations since during this process, the energy of the inflaton is transferred to the thermal energy of the particles [13]. These particles interact and will eventually thermalise to equilibrium at a reheating temperature, $T_r$, which varies according to the inflationary model [15]. Once all the energy of the inflaton is transferred to the particles, reheating ends and the Universe starts its well known radiation era. The details of reheating are very complicated and very sensitive to its inflationary background, choice of parameters and initial conditions. In most inflationary models, it was found that reheating is made of distinct stages that have extremely different features, the first called preheating and the second of thermalization.

As mentioned above, reheating very much depends on the choice of the inflationary scenario. The model I am interested to study in this thesis is a model in which matter is *non-minimally* coupled to gravity [16]. First of all, what is non-minimal coupling? Consider a general theory described by the action [17],

$$S = \int d^4x\sqrt{-g}\left[\frac{1}{2\kappa}R + \mathcal{L}_m\right], \tag{1.3.1}$$

where $\kappa \equiv 8\pi G$, R is the Ricci scalar and $g \equiv det(g_{\mu\nu})$. The first term is the Einstein-Hilbert term which yields the gravitational field equations and it therefore describes the gravitational part [18], while $\mathcal{L}_m$ describes the matter sector of the system. These two parts do not interact and are said to be minimally coupled. However, there is nothing preventing gravity and matter to interact and it seems rather natural for them to be coupled [19]. Therefore, I chose to study a more realistic model in which the gravitational sector and the matter sector are not two distinct parts of the action but are instead coupled in a non-minimal manner. In particular, I chose the non-minimal coupling term between curvature and the inflaton $\phi$ to be of the form, $\xi R\phi^2$. I will study the effect of this term on the reheating process by comparing two systems driven by the same potential, one minimally-coupled and the other non-minimally coupled to gravity.

## 1.4 Gravitational Waves

The second part of this thesis focuses on the production of gravitational waves during reheating. Gravitational waves are ripples in the curvature of

space-time that travel at the speed of light [20]. Generally, they are formed due to accelerating massive objects which deform the spacetime. Spacetime then must change in order to adapt to its new position. In fact, as the physicist John Wheeler said, "*Matter tells space how to curve, space tells matter how to move*". These distortions of spacetime which propagate as waves at the speed of light are what we call gravitational waves.

They were predicted by Einstein in 1916 [21] and were one of the greatest achievements of his theory of General Relativity. In 1918, he presented for the first time a full calculation of its effects, using his famous "quadrupole formula" [22]. One may tempt to draw an analogy between electromagnetic waves and gravitational waves. However, their nature is significantly different. In fact, electromagnetic waves propagate through spacetime oscillating, while gravitational waves are propagating distortions of the spacetime itself.

Gravitational waves are generated by distortions in spacetime of astrophysical and cosmological origin [4]. The nature of gravitational waves varies with the process which generated it. This results in distinct gravitational backgrounds being formed depending on the conditions of their origin [23]. In this thesis, I will restrict my interest to the gravitational wave background produced during reheating after chaotic inflation. Unfortunately, today's gravitational wave observatories such as LIGO or (future) LISA are only sensible to certain astrophysical gravitational waves since those of cosmological origins are well below their frequency range [24].

Since the CMB fluctuations were detected, cosmologists have been able to study primordial perturbations. During inflation gravitational waves are generated from tensor perturbations of the metric, while scalar perturbations generate density perturbations (and hence the whole structure of the Universe). These perturbations are being detected on the CMB by observatories such as Planck and they provide constraints on inflationary models [25]. However, CMB measurements are not enough to rule out a single inflationary model in agreement with the data. Recently, direct detection of B-Modes by the BICEP2 observatory based on the South Pole may have given further constraints on inflation but its reliability is questionable due to ground dust inconsideration [26].

Instead, how much would we know of the early Universe if gravitational waves were to be detected directly? One feature that makes gravitational waves particularly interesting is that once they are formed they immediately decouple [27]. This means that the gravitational waves filling our Universe have been freely propagating since the instant they were formed. This is a unique feature of these kind of waves. In this way, they carry direct and unperturbed information about their origin and the dynamical process which generated them. This is the reason why if gravitational waves of cosmological origin were to be detected, they would provide an enormous contribution to our understanding of the early Universe.

In particular, the detection of gravitational waves produced during re-

heating would allow us to have a direct signature of the inflationary potential, the particle's couplings and the inflaton's nature. In other words, it would be a most reliable tool to study Inflation and recover further constraints on the model responsible for it. One may even think that gravitational waves may be the only way for cosmologists to finally solve the mysteries of the early Universe.

For this reason I chose to analyse both the theoretical aspect of the theory of reheating itself aswell as its gravitational wave imprint. Via numerical lattice simulations, I will be predicting the gravitational wave spectra generated during reheating by the quartic chaotic model non-minimally coupled to gravity, on which I am concentrating my whole discussion on.

## 1.5 Outline of the thesis

In Chapter 2, I will focus on inflation and show how it originated in order to solve three cosmological puzzles. I will review its phenomenology and discuss how quantum inhomogeneities arise from this era. This discussion sets the mathematical and theoretical basis for the next chapter.

Chapter 3 will focus on one of the main subjects of this thesis; the reheating era of the Universe. I will discuss the Universe's transition from inflation to reheating and derive in detail the phenomenological process of preheating. To study its non-linear dynamics, I will perform numerical lattice simulations using a modified version of the publicly available C++ LatticeEasy package. I will focus on a quartic chaotic inflationary model involving an inflaton interacting with another light scalar field. I will compare the dynamics of reheating in this model for both cases of minimal and non-minimal coupling between the fields and gravity.

In chapter 4, I will discuss the production of gravitational waves during reheating. At first I will discuss how gravitational waves can be detected and their role in our understanding of the Universe. I will derive the equation for the energy specrum analytically and give numerical results using a further modified version of LatticeEasy. Again, I will focus on the same chaotic model in both cases of minimal and non-minimally coupling to gravity.

In chapter 5 I will present some ideas on how my work can be improved in the future and how this could both increase the accuracy of my results and further analyse its implications.

Finally in chapter 6, I will draw conclusions on the results that I found from both my analytical and numerical computations and discuss the significance of these for the development of this area of research.

# 2. Inflation

In this chapter, we review the key theoretical concepts of inflation required to study the following stage of reheating. We first review the main concepts of the hot Big Bang theory and the historical origin of inflation. Next, we will briefly show how inflation theory solves the horizon, flatness and magnetic monopole problems arising from the hot Big Bang model.

I wil present the dynamics of the Universe (seen as homogenous and isotropic) at the very beginning of its life as described by the theory of inflation. For completeness, I will take into account its non-isotropic nature and show perturbations of the metric decompose into scalar, vector and tensor components.

## 2.1 From the Hot Big Bang to Inflation

Before inflation was even ever mentioned, the origin of the Universe was described by the hot Big Bang theory. The hot Big Bang theory relies on the *Cosmological Principle*, which states that the properties of Universe at sufficiently large scale are the same for all observers [3]. In other words, the distribution of matter in the Universe is homogeneous and isotropic when viewed on a large enough scale.

The metric which describes such a spacetime is the Friedmann–Lemaître–Robertson–Walker(FLRW) metric [28],

$$ds^2 = -dt^2 + a^2(t)\left[\frac{dr^2}{1-kr^2} + r^2\left(d\theta^2 + \sin^2\theta d\phi^2\right)\right], \tag{2.1.1}$$

where $a(t)$ is the scale factor, which describes its physical size and $k$ measures the spatial curvature ($k = -1, 0, 1$ if spacetime is open, flat or closed respectively). For the purposes of this thesis, we will be mainly dealing with flat FLRW spacetime metric, $ds^2 = -dt^2 + a^2(t)[dx^2 + dy^2 + dz^2]$, in Cartesian comoving coordinates.

General Relativity was the first theory to dictate a strict correlation between gravity and the geometry of spacetime [17]. This relationship is described by the Einstein equations [21],

$$G_{\mu\nu} = 8\pi G T_{\mu\nu}, \tag{2.1.2}$$

where $G_{\mu\nu} \equiv R_{\mu\nu} - \frac{1}{2} g_{\mu\nu} R$, $R_{\mu\nu}$ is the Ricci tensor, $R$ is the Ricci scalar and $T_{\mu\nu}$ is the stress energy-momentum tensor. The assumption of a homogenous and isotropic Universe yields a stress energy-momentum tensor of the form [29],

$$T_{\mu}{}^{\nu} = diag[-\rho(t), P(t), P(t), P(t)], \tag{2.1.3}$$

where $\rho$ is the energy density and $P$ is the pressure. The main equations describing the expansion of the Universe can be derived by the 00 and $ij$ components of the Einstein equations, which imply the so called Friedmann equations,

$$H^2 \equiv \left(\frac{\dot{a}}{a}\right)^2 = \frac{8\pi G}{3}\rho - \frac{k^2}{a^2}, \tag{2.1.4}$$

$$\frac{\ddot{a}}{a} = \dot{H} + H^2 = -\frac{4\pi G}{3}(\rho + 3P). \tag{2.1.5}$$

They can be combined to give a third equation, known as the continuity equation,

$$\dot{\rho} + 3H(\rho + P) = 0. \tag{2.1.6}$$

The standard hot Big Bang theory describes those epochs of the Universe where it is cool enough and all the physical processes are fairly understandable via experiments. Unfortunately, it does not cover the first moments after the Universe was created.

Inflation is the most accepted theory of the very early Universe. Inflation is a general term for models which predict a phase of accelerated expansion, blowing the size of the Universe up from a region smaller than a proton in only a few fractions of a second. From the Friedmann equation (2.1.5), one can see that $\ddot{a} > 0$ requires [30],

$$\rho + 3P > 0 \implies P < -\frac{\rho}{3}. \tag{2.1.7}$$

Thus, the type of matter driving inflation must have negative pressure. This seems quite unusual; what kind of matter can satisfy this? The cosmological constant is a first example which would satisfy such an equation of state. The cosmological constant, $\Lambda$, was first introduced by Einstein in 1917 and it is associated with the vacuum energy density of the Universe. Its equation of state satisfies the relation $P = -\rho$ [4]. For this reason, it seemed as a plausible candidate for inflation.

However, if inflation was led by a cosmological constant, inflation would be lasting forever and the Universe would never be entering the radiation

era. This option can therefore be excluded quite straightforwardly. A more plausible explanation is that responsible for this enormous expansion is some scalar field, the *inflaton*, which carries all the energy of the Universe during inflation [9]. The behaviour of the inflaton driving the expansion depends on the details of the inflationary model. So far, physicists do not agree on a unique model which can describe every aspect of inflation and its successive eras.

The first realistic and physical model of inflation was developed by Alan Guth in 1981 [31]. His model, known as *old inflation*, predicted a Universe in a supercooled false vacuum state which underwent an exponential expansion making it very big and flat. A false vacuum state is a state of large energy density in which no matter is present. The false vacuum would then decay and the Universe would become hot. Even though the physics of his model turned out to be incorrect, it was the first theory which was able to solve the standard Big Bang theory problems.

In 1981-1982, *new inflationary theory* was developed. The difference with old inflation is that the Universe could have started in a false vacuum or in an unstable state at the top of a very flat potential [9]. The inflaton field, the field carrying all the energy, slowly rolls away from the false vacuum on the flat potential until it falls down to its minimum. This is why this theory is also called *slow-roll* inflation. Again the physics of it implied initial conditions which were not quite correct. For instance, in this theory there was still the assumption that the Universe must have started in thermal equilibrium. Hence, both old and new inflation resulted to be incomplete theories. However, they played a fundamental role in the development of Cosmology thanks to the new revolutionary ideas they scattered amongst cosmologists.

In 1983, *chaotic inflation* was developed [12]. The evolution of the inflaton during inflation is described in the same way as in new inflation theory. However, according to this theory, the slow-roll regime could have occurred even if the Universe was not initially in thermal equilibrium, which was one of the main limits of old and new inflation. Furthermore, chaotic inflation is a theory which can be applied to *any* form of potential, as long as it is enough flat to allow slow-roll to occur. Chaotic inflation theory was the first realistic inflationary model which occurred under rather natural initial conditions. It is based on chaotic initial conditions in the very early Universe which seems as a natural assumption since there were no correlation between physical processes in different regions of space. Under this assumption, at planck time $t \sim t_{pl} \sim M_{pl}^{-1}$, there exists a sufficiently isotropic and homogenous spacetime of size larger than $M_{pl}$ filled with a homogenous field $\phi \gtrsim M_{pl}$ [12]. The field $\phi$ has no *a priori* initial condition and may take any arbitrary

value between $-\infty$ and $\infty$ in different regions of the Universe. In particular, values of $\phi \gg M_{pl} \sim 10^{19}$ GeV are reasonably legitimate. The only possible constraint on the field $\phi$ is that $(\partial_\mu \phi)^2 \ll M_{pl}^4$. This condition is connected to the condition $V(\phi) \lesssim M_{pl}^4$ which should be satisfied since otherwise the Universe would enter a pre-planckian era in which space and time are not classically defined [9].

## 2.2 Cosmological puzzles

The idea of inflation arose to solve phenomena which the Big Bang theory could not solve [32]. The Big Bang model implied certain initial conditions for which three observations would be theoretically impossible.

**The Horizon problem**

The first involves observations of the Cosmic Microwave Background (CMB). As mentioned in the introduction, the CMB is a radiation background filling the Universe which originated in the recombination era at the time of photon decoupling. A soon as photons decoupled, they started to free-stream from the so called *surface of last scattering*. The temperature of this radiation, $T \sim 2.7K$ is isotropic to better than 1 part in $10^5$. This could be naturally explained if different regions of the Universe have been able to interact and reached thermal equilibrium.

However, according to hot Big Bang cosmology, photons from different regions of the universe should not have had sufficient time to have come in contact with each other by the time they started free-streaming. In other words, they were outside each other's past lightcones, or they were *causally disconnected*, and therefore had no way to communicate. However, the quasi isotropic and homogenous nature of the CMB implies that there has been exchange of information between those regions, which raises a contradiction [30]. This is called the *horizon problem*; The problem of understanding why causally disconnected regions in the cosmic microwave background have effectively the same temperature.

In order to analyse this problem in more detail, let me introduce the concept of *comoving particle horizon* [33]. The comoving particle horizon is the maximum distance travelled by a photon from an initial time $t = 0$ to a final time $t$. Since photons follow null geodesics, i.e. $ds^2 = 0 = -dt^2 + a(t)^2 dr^2$, the particle's horizon is mathematically defined as,

$$R_H(t) = \int_0^t \frac{dt'}{a(t')}. \tag{2.2.1}$$

In general, for $a \sim a_0 \, (t/t_0)^p$,

$$R_H(t) = \frac{p}{1-p}\left(\frac{1}{Ha}\right)\Big|_t . \tag{2.2.2}$$

The comoving particle horizon sets the causal size of a region in the sense that points in space at a distance larger than the comoving horizon are necessarily causally disconnected. This means that they have non-intersecting past light cones and that they have never interchanged information.

The horizon problem arises since the comoving particle horizon at recombination, $\tau^\star$, is smaller than the comoving radius of the last scattering surface, $r_{lss}$, i.e. the comoving distance light has travelled after recombination. Assume that the Universe is matter dominated so that $a = a_0(t/t_0)^{2/3}$ and $H = \frac{2}{3}t^{-1}$, where the subscript 0 denotes quantities to evaluate today and we normalize $a_0 = 1$. Thus, using (2.2.2), the comoving distance a photon has travelled under these conditions at a scalar factor $a$ is,

$$R_H(t) = \frac{2}{H_0}\sqrt{a}. \tag{2.2.3}$$

At the surface of last scattering, $a \approx 1100$. Therefore, the comoving particle horizon at recombination was $\sqrt{1100}$ times smaller than today's. It is therefore surprising that regions causally disconnected at recombination happen to be nearly at the same temperature today.

Including a period of inflation can solve this contradiction [32]. It is useful to rewrite the particle's horizon as,

$$R_H = \int_0^{a_0} da \frac{1}{Ha^2} = \int_0^{a_0} d(\ln a)\frac{1}{Ha}, \tag{2.2.4}$$

where $1/Ha$ is known as the *comoving Hubble radius*. The comoving Hubble radius is another way to measure whether particles are causally connected to each other at a certain value of the scale factor $a$; if they are separated by distances larger than the Hubble radius then they cannot communicate with each other. The particle horizon instead, tells us if two points have ever been in causal contact in the past.

During radiation or matter dominated era, the comoving Hubble radius increases monotonically and it is proportional to $R_H$. If there was a phase in which the comoving Hubble radius decreased, the particle horizon could still grow but the causally connected regions at the end of this phase would be smaller than they were originally.

Furthermore, the particle horizon increases dramatically as the comoving Hubble radius decreases. Therefore, at recombination, the particle horizon is larger than the distance travelled by the photons since then. Hence, the photons from the CMB come from a region which is within its physical horizon and which allows them to reach thermal equilibrium.

In order to have a decreasing comoving Hubble radius, we must impose,

$$\frac{d}{dt}(aH) = \frac{d}{dt}\left(a\frac{da/dt}{a}\right) = \frac{d^2a}{dt^2} > 0. \tag{2.2.5}$$

Hence, we found that such a phase require an accelerated expansion. The second Friedmann equation,

$$\frac{\ddot{a}}{a} = -\frac{4\pi G}{3}(\rho + 3P), \tag{2.2.6}$$

tells us that for $\ddot{a} > 0$, one needs $p < -\frac{\rho}{3}$, i.e. a form of matter with negative pressure. Inflation satisfies these requirements and can therefore solve the horizon problem.

**The Flatness problem**

The second cosmological puzzle is related to observations on the curvature of the Universe today. The question simply is, why is the Universe today so flat? The curvature of the Universe today results to be very small [29]. From general relativity, we know that spacetime can be open, closed or flat. No constraint has been set for which our Universe has to be spatially flat. Indeed if initially it was not, the fact that it is so close to flatness today seems rather unnatural. In an expanding Universe, assuming conditions for matter era, the curvature should be increasing; this implies that initially it would have been even tinier than today. Let me define the critical density, $\rho_c$, as the energy density of a flat FLRW spacetime,

$$\rho_c = \frac{3H^2}{8\pi G}. \tag{2.2.7}$$

We can give an estimate of the curvature by defining a density parameter $\Omega$ such that [34],

$$\Omega = \frac{\rho}{\rho_c}, \tag{2.2.8}$$

where $\Omega = -1, 0, 1$ corresponds to an open, flat and closed Universe, respectively. From these definitions, notice that one can rewrite the first Friedmann equation (2.1.4) in terms of the critical density as,

$$H^2 = H^2\Omega - \frac{k^2}{a^2}. \tag{2.2.9}$$

Finally, this yields the useful relation,

$$\Omega_k = \Omega - 1 = \frac{k}{a^2H^2}. \tag{2.2.10}$$

We can see that if $\Omega = 1$ then it will remain so but if $\Omega \neq 1$, it will evolve since the scale factor decreases with time. One can estimate that the density

parameter today $\Omega_K(t_0) < 0.02$ for $t_0 \simeq 10^{17}$ seconds and that at Planck's time $t_{pl} = 10^{-43}$ seconds, $\Omega_K(t_{pl}) < 10^{-61}$.

Inflation solves this problem since during inflation curvature decreases drastically [31]. This is due to the rapid exponential expansion which flattens out the Universe. During inflation the scalar factor increases exponentially and hence, from equation (2.2.10) we see that $\Omega_k$ decreases very rapidly and $\Omega \to 1$. Thus, it is the intrinsic nature of inflation which brings the Universe to tend to flatness. In this way, the initial condition for the curvature needs not to be unnaturally small and the problem is solved.

**Monopole problem**

A third observation was related to visible defects of our Universe today, such as magnetic monopoles, domain walls and strings. Particles theories predict the creation of topological defects due to phase transitions [4]. Phase transitions are a consequence of symmetry breaking occurring in particle models.

Magnetic monopoles are the most prevalent in particle theories. The problem is that although theories predict a very large number of magnetic monopoles produced for instance by electroweak symmetry breaking, we do not see them. This problem can be explained by inflation. In the early Universe, defects were created at a density of order $\sim 1$ per Hubble volume, i.e. one per each observable Universe. Inflation, due to its exponential expansion, dilutes the density of the monopoles since it stretches all lengths by a factor of $\sim 10^{26}$ [33]. Hence, one monopole per Hubble volume actually becomes one every $10^{60}$ horizon volumes, explaining why magnetic monopoles have not been detected in our observable Universe.

## 2.3 Slow-roll inflation

As mentioned before, inflation occurs under a slow-roll regime of the inflaton. This means that during inflation, the inflaton slowly rolls on a very flat potential and this drives the Universe to expand exponentially (figure 2.3.1) [9]. The slow-roll regime must last a finite amount of time during which the Universe exponentially expands for long enough. At the end of the slow-roll regime, the inflaton rolls down to the minimum of its potential and inflation ends. At this stage, the inflaton starts oscillating around the minimum and the process of reheating begins.

The action of a scalar field in flat FLRW spacetime is given by [35],

$$S = -\int dt d^3x \sqrt{-g}\left(\frac{1}{2}\partial_\mu\phi\partial^\mu\phi + V(\phi)\right), \tag{2.3.1}$$

where $g \equiv det(g_{\mu\nu})$ and $V(\phi)$ is the potential of the scalar field. By varying the action with respect to $\delta\phi$ we can recover the equations of motion

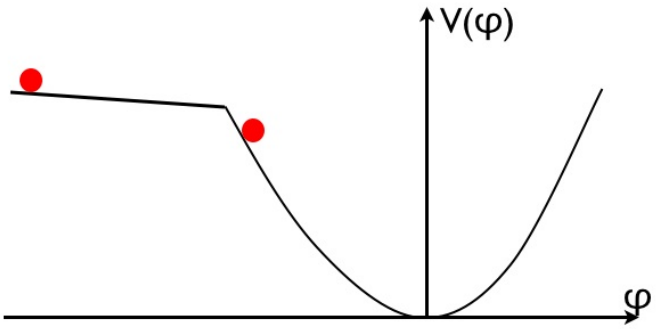


**Figure 2.3.1:** Graph of a typical potential of the inflaton field

of the scalar field in an FLRW spacetime given by the metric (2.1.1),

$$\ddot{\phi} + 3H\dot{\phi} - \frac{1}{a^2}\nabla^2\phi + V'(\phi) = 0. \tag{2.3.2}$$

Notice that the second term in the equation above, the Hubble damping, is a new unusual term. It acts as a damping term which arises due to taking into account the expansion of the Universe.

The stress-energy tensor for a scalar field is given by,

$$T_{\mu\nu} = \partial_\mu\phi\partial_\nu\phi - g_{\mu\nu}\left(\frac{\partial^\sigma\phi\partial_\sigma\phi}{2} + V(\phi)\right), \tag{2.3.3}$$

where the 00 component $T_{00} = \rho$ and the $ij$ component $T_{ij} = a^2 P\delta_{ij}$. Hence, we derive expressions for the energy density and pressure, respectively,

$$\rho = \frac{\dot{\phi}^2}{2} + V(\phi), \tag{2.3.4}$$

$$P = \frac{\dot{\phi}^2}{2} - V(\phi). \tag{2.3.5}$$

Finally, the Friedmann equations (2.1.4) and (2.1.5) are given by,

$$H^2 = \frac{8\pi G}{3}\left(\frac{1}{2}\dot{\phi}^2 + V(\phi)\right), \tag{2.3.6}$$

$$\dot{H} = -4\pi G\dot{\phi}^2. \tag{2.3.7}$$

The evolution of the scalar field is fully described by the Klein-Gordon equation (2.3.2) and the Friedmann equations (2.3.6) and (2.3.7).

One necessary condition of inflation is that the inflaton must have negative pressure, $P < -\rho/3$. Here, this is equivalent to the condition $\dot{\phi}^2 < V(\phi)$. Hence, during inflation the potential energy dominates the kinetic energy

and the expansion is accelerated. Thus, in order for the energy density to be dominated by the potential energy, inflation requires the first slow-roll condition [9],

$$\dot{\phi}^2 \ll V(\phi). \tag{2.3.8}$$

The second condition assures that the Hubble damping term dominates the field equation of motion in order for the field $\phi$ to be rolling very slowly on the flat solpe of the potential before reaching its minimum $\phi = 0$. To have this, in equation (2.3.2), the damping term must be dominating over the double time derivative of the field. This condition is known as the second slow-roll condition and it is given by [30],

$$|\ddot{\phi}| \ll H|\dot{\phi}|. \tag{2.3.9}$$

Applying the slow-roll conditions to the Friedmann equations, we recover the approximate expression, $H^2 \approx \frac{8\pi G}{3}V(\phi)$ and $3H\dot{\phi} \approx -V'(\phi)$. Furthermore, the second Friedmann equation (2.3.7) becomes $\dot{H} \simeq 0$. This last expression is easily solvable and it implies $a \approx Ae^{Ht}$, where A is a constant. Here we have proved that in fact inflation is driven by an exponentially rapid expansion and it is effectively a De Sitter phase.

A more convenient way to express the slow-roll conditions is via two dimensionless slow-roll parameters conventionally defined as [34],

$$\epsilon \equiv \frac{1}{16\pi G}\left(\frac{V'}{V}\right)^2, \qquad \eta \equiv \frac{1}{8\pi G}\left(\frac{V''}{V}\right). \tag{2.3.10}$$

Consider the two parameters to be small, i.e. $\epsilon \ll 1$ and $\eta \ll 1$ [36]. From the definitions of $\epsilon$ and $\eta$ above, one obtains the following inequalities,

$$\left(\frac{V'}{V}\right)^2 \ll 16\pi G, \tag{2.3.11}$$

$$\left(\frac{V''}{V}\right) \ll 8\pi G. \tag{2.3.12}$$

Recall that following the slow roll conditions, we have derived the approximate Friedmann equation $V'(\phi) \approx -3H\dot{\phi}$. Thus, by substituting this in equation (2.3.11), one obtains,

$$\frac{9H^2\dot{\phi}^2}{V^2} \ll 16\pi G \implies \frac{24\pi G V\dot{\phi}^2}{V^2} \ll 16\pi G \implies \dot{\phi}^2 \ll V, \tag{2.3.13}$$

where for the first implication I have used the second approximate Friedmann equation $H^2 \approx \frac{8\pi G}{3}V(\phi)$. Hence, we have derived the first slow-roll condition (2.3.8) from the assumption $\epsilon \ll 1$.

Now consider the approximate Friedmann equation $\dot{\phi} \approx -\frac{V'(\phi)}{3H}$ and differentiate it with respect to time. One obtains,

$$\left|\ddot{\phi}\right| \approx \left| -\frac{V''\dot{\phi}}{3H} + \frac{V'}{3}\left(\frac{\dot{H}}{H^2}\right)\right| \approx \left| -\frac{V''\dot{\phi}}{3H}\right|, \tag{2.3.14}$$

since $\dot{H}/H^2 \approx -3\dot{\phi}^2/2V \ll 1$ from the first slow-roll condition derived in (2.3.13). Now we divide both sides of the equation by H and obtain,

$$\left|\frac{\ddot{\phi}}{H}\right| \approx \left|\frac{-V''\dot{\phi}}{3H^2}\right| \approx \left| -\frac{V''\dot{\phi}}{8\pi GV}\right| \ll \left|\dot{\phi}\right|, \tag{2.3.15}$$

where for the second equality I used again the Friedmann equation $H^2 \approx \frac{8\pi G}{3}V(\phi)$ and for the last step I used the assumption $\eta \ll 1$. Thanks to this assumption, we have recovered the second slow-roll condition of equation (2.3.9).

In conclusion, the two slow-roll conditions can be summarized in the simpler forms $\epsilon \ll 1$ and $\eta \ll 1$. These expression can be interpreted as requiring the curvature and the slope of the potential to be sufficiently small.

A useful quantity that one can measure is the "amount" of inflation that the Universe underwent, the *number of e-foldings*. It is defined as the logarithmic amount of expansion during the slow-roll regime. This quantity depends strictly on the potential which drives the inflaton. The number of e-foldings is defined as [33],

$$N = \ln\left(\frac{a_2}{a_1}\right) = \int_t^{t_{end}} H dt = H\int_\phi^{\phi_{end}} \frac{1}{\dot{\phi}} d\phi \approx -\int_\phi^{\phi_{end}} 8\pi G \frac{V(\phi)}{V'(\phi)} d\phi, \tag{2.3.16}$$

where $a_2$ and $a_1$ are values of the scale factor at the end and at the start of slow-roll inflation, respectively. By definition, N decreases during inflation until it reaches zero at the end of inflation. The number of e-folds is a constraint which assures that inflation lasts long enough. According to observations, the largest scales observed today, the CMB scales, leave the horizon $N_{star} \sim 60$ before the end of inflation.

Moreover, one can estimate the value of the field at the end of inflation, which results to be the value for which either one of the slow roll parameters $\epsilon$ or $\eta$ equals to 1. Thus, e-folds can also be used to estimate the value of the field $\phi_\star$ for which it leaves the horizon, after a sufficient number of e-folds.

For instance, take chaotic inflation with the potential $V(\phi) = \frac{1}{2}m^2\phi^2$. The slow-roll parameters $\epsilon = \eta = 2M_{pl}^2/\phi^2$ are small only for large values of $\phi$, i.e. $\phi > \sqrt{2}M_{pl} \equiv \phi_{end}$. Hence, inflation occurs for very large value of the field and ends once $\epsilon \sim 1$ and $\phi_{end} \sim 2M_{pl}$. Observable scales leave the horizon at $N_\star \sim 60$, where $N_\star$ is given by,

$$N_\star = \int_{\phi_{end}}^{\phi_\star} \frac{\phi}{2} d\phi \approx \frac{\phi_\star^2}{4M_{pl}^2}. \tag{2.3.17}$$

Hence, observable scales leave the horizon at $\phi_\star \approx \sqrt{4 \times 60} M_{pl} \approx 15 M_{pl}$.

## 2.4 Inhomogeneities from inflation

So far, we have considered the Universe to be homogenous and isotropic. This consideration is not complete to account for real cosmology. One must must also study deviations from isotropy and homogeneity. Inflation was firstly formulated in order to solve the cosmological problems mentioned in section 2.2. Later on, cosmologists realised that as a theory itself it could explain the origin of the inhomogeneities and hence the large structure of the Universe [30].

Cosmological inhomogeneities are a consequence of quantum fluctuations of matter and metric perturbations during inflation. The most relevant matter fluctuation is that of the inflaton, which sources both the CMB temperature fluctuations and structure formation. Thus, for simplicity, I will assume matter is made up of a single real scalar field.

Consider a perturbed inflaton field living in a perturbed spacetime geometry. Einstein's equations tell us that field perturbations and metric perturbations must coexists. Thus, expand the inflaton field and the metric such that,

$$\phi(t, \mathbf{x}) = \bar{\phi}(t) + \delta\phi(t, \mathbf{x}), \qquad g_{\mu\nu}(t, \mathbf{x}) = \bar{g}_{\mu\nu}(t) + \delta g_{\mu\nu}(t, \mathbf{x}), \tag{2.4.1}$$

where $\bar{\phi}(t)$ and $\bar{g}_{\mu\nu}$ drive the homogenous background and $\delta\phi(t, \mathbf{x})$ and $\delta g_{\mu\nu}(t, \mathbf{x})$ generate the perturbations. The perturbation components must be small, such that $\delta g_{\mu\nu}(t, \mathbf{x}) \ll 1$ and $\delta\phi(t, \mathbf{x}) \ll \bar{\phi}(t)$.

In principle, the 4x4 symmetric tensor $\delta g_{\mu\nu}(t, \mathbf{x})$ carries ten degrees of freedom [34]. These correspond to either scalar, vector or tensor perturbations according to their properties with respect to spatial rotations.

Scalar perturbations are invariant under spatial rotations and they are the principal source of anisotropies and inhomogeneities of the Universe. Vector and tensor perturbations transform as vectors and tensors under rotations. Vector perturbations arise from rotational velocity fields and tensor perturbations generate gravitational waves. There are four scalar, four vector and two tensor degrees of freedom. At first order in perturbation theory, these degrees of freedom obey their own equation of motion and hence can be treated separately [2]. This is called the SVT decomposition.

Expanding the first derivative of the potential, such that $V'(\phi) = V'(\phi_{cl}) + \delta\phi V''(\phi_{cl})$, and substituting it in the equation of motion (2.3.2) together with the expansion of $\phi$, one obtains the equation of motion for fluctuations $\delta\phi$,

$$\delta\ddot{\phi} + 3H\delta\dot{\phi} - \frac{1}{a^2}\delta^{ij}\partial_i\partial_j\delta\phi + V''(\phi_{cl})\delta\phi = 0. \tag{2.4.2}$$

The vector degrees of freedom describe gravito-magnetism and the have only decaying solutions; its analysis is therefore neglectable. The scalar degrees of freedom generalize Newtonian gravity and are coupled to the field perturbation $\delta\phi$. Tensor perturbations are instead decoupled from the field and they describe gravitational waves.

One subtle point to make is that the metric perturbation has more degrees of freedom than the true physical degrees of freedom of the system [37].This fact is related to gauge transformations which create extra non-physical degrees of freedom. Gauge transformations in general relativity are generic coordinate transformations from one frame to another. The gauge abundance comes from the fact that there is no preferred coordinate system and hence there is freedom of choice. Thus, one must fix the gauge in order to choose a coordinate system. Gauge transformations have 4 degrees of freedom and hence we find that the physical degrees of freedom are $10 - 4 = 6$; two scalar, two vector and two tensor degrees of freedom. For the purpose of this thesis, I will focus on tensor perturbations. For discussions on scalar perturbations, see [29], [35].

**Power spectrum**

Let me first define in general the notion of a power spectrum. It is defined as the ensemble average over fluctuations and it describes the amplitude of the k-modes of a field $\phi$ [35],

$$\langle\phi_{\mathbf{k}}\phi_{\mathbf{k}'}\rangle = (2\pi)^3\delta(\mathbf{k}+\mathbf{k}')P_\phi(k). \tag{2.4.3}$$

One can also define a dimensionless power spectrum $\mathcal{P}$, such that

$$\mathcal{P} = \frac{k^3}{2\pi^2}P_\phi(k). \tag{2.4.4}$$

A statistical measure of primordial scalar fluctuations is the power spectrum of $\mathcal{R}$, the comoving curvature perturbation which describes the spatial curvature of comoving hypersurfaces. The power spectrum is given by,

$$\langle\mathcal{R}_{\mathbf{k}}\mathcal{R}_{\mathbf{k}'}\rangle = (2\pi)^3\delta(\mathbf{k}+\mathbf{k}')P_{\mathcal{R}}(k) \qquad \mathcal{P} = \frac{k^3}{2\pi^2}P_{\mathcal{R}}(k). \tag{2.4.5}$$

Furthermore, once can quantise the scale-dependence of the power spectrum via the scalar spectral index $n_s$, such that [29],

$$n_s - 1 \equiv \frac{d\ln\mathcal{P}_{\mathcal{R}}}{d\ln k}. \tag{2.4.6}$$

Similarly for the tensor perturbations, the power spectrum of the two polarization modes of gravitational waves (+, x), corresponding to the perturbations' two degrees of freedom, is defined as [35],

$$\langle h_{\mathbf{k}} h_{\mathbf{k}'} \rangle = (2\pi)^3 \delta(\mathbf{k} + \mathbf{k}') P_h(k) \qquad \mathcal{P}_h = \frac{k^3}{2\pi^2} P_h(k). \tag{2.4.7}$$

Thus, the full power spectrum of the tensor perturbations is defined as the sum of the contributions from each polarization mode, i.e. $\mathcal{P}_t = 2\mathcal{P}_h$. As for scalar perturbations, one can define the tensor spectral index $n_t$ [29],

$$n_t \equiv \frac{d \ln \mathcal{P}_t}{d \ln k}. \tag{2.4.8}$$

In the next section, I will show how quantum fluctuations during inflation are the source of the scalar and tensor primordial power spectra, $\mathcal{P}_s(k)$,$\mathcal{P}_t(k)$.

### 2.4.1 Quantum fluctuations

Quantum fluctuations are generated on all length scales but we are interested in subhorizon modes, i.e. those inside the Hubble radius where $k \gg aH$. Recall that during inflation the comoving Hubble radius $(aH)^{-1}$ shrinks but all other comoving scales such as k . Hence, fluctuations will eventually exit the horizon, where $k > aH$. Once this happens, fluctuations can be described by a classical probability distribution with variance given by the power spectrum evaluated at the horizon crossing due to the De Sitter expansion stretching modes to very large scales [3]. After inflation, the comoving horizon will start growing again and eventually the fluctuations will re-enter the horizon. We will not need to worry about their behaviour while outside the horizon since in that scenario, no causal physics takes place.

In this section, I will briefly derive the power spectrum of tensor fluctuations and state the main results derived in [35] on scalar perturbations and spectral indices.

Tensor perturbations are gauge invariant, i.e. they don't change under gauge transformations. Gravitational waves are described by the two independent components of the 3x3 transverse traceless tensor $h_{ij}$ such that,

$$\delta g_{ij} = -a(\eta)^2 h_{ij}, \tag{2.4.9}$$

where $\eta$ is conformal time. Moreover, the tensor $h_{ij}$ can be decomposed such that,

$$h_{ij} = h_1 e^1_{ij} + h_2 e^2_{ij}, \tag{2.4.10}$$

where $h_1$ and $h_2$ are the two degrees of polarization of gravitational waves(+,x) and $\epsilon^1_{ij}$ and $\epsilon^2_{ij}$ are two orthogonal transverse traceless tensors.

By expanding the Einstein-Hilbert action, we obtain the action of the gravitational waves in the linear approximation, given by

$$S = \frac{1}{8\kappa^2}\int d\tau d^3x a^2 \left[\left(\partial h'_{ij}\right)^2 - \left(\partial_l h_{ij}\right)^2\right]. \tag{2.4.11}$$

To simplify calculations, I will define the following expansion [35],

$$h_{ij} = \int \frac{d^3k}{(2\pi)^3}\sum_{s=+,x}\epsilon^s_{ij}(k)h^s_{\mathbf{k}}(\tau)e^{i\mathbf{kx}}, \tag{2.4.12}$$

where $\epsilon_{ii} = k^i\epsilon_{ij} = 0$ and $\epsilon^s_{ij}(k)\epsilon^{s'}_{ij}(k) = 2\delta_{ss'}$. Thus, the tensor action becomes

$$S = \sum_s \int d\tau d\mathbf{k}\frac{a^2}{4\kappa^2}\left[h^{s\,\prime}_{\mathbf{k}}h^{s\,\prime}_{\mathbf{k}} - k^2 h^s_{\mathbf{k}}h^s_{\mathbf{k}}\right]. \tag{2.4.13}$$

By making a further redefinition such that $v^s_{\mathbf{k}} \equiv \frac{a}{2}\kappa h^s_{\mathbf{k}}$, we recover the action in the simple form,

$$S = \sum_s \frac{1}{2}\int d\tau d^3\mathbf{k}\left[(v^{s\,\prime}_{\mathbf{k}})^2 - \left(k^2 - \frac{a''}{a}\right)(v^s_{\mathbf{k}})^2\right]. \tag{2.4.14}$$

This yields the equation of motion for a massless field in De-Sitter space-time. Thus, the two polarization of gravitational waves can be seen as renormalized massless fields in De-Sitter space [35],

$$h^s_{\mathbf{k}} = \frac{2\kappa}{a}\psi_{\mathbf{k}}, \qquad \text{with} \qquad \psi_{\mathbf{k}} = \frac{v_{\mathbf{k}}}{a}. \tag{2.4.15}$$

The detailed calculation of the power spectrum of $\psi$ is shown in [35]. From that, once can deduce the power spectrum of a single polarization of tensor perturbations. The result in terms of dimensionless power spectrum is given by,

$$\mathcal{P}_h(k) = 4\kappa^2\left(\frac{H_\star}{2\pi}\right)^2, \tag{2.4.16}$$

where $H_\star$ is the value of $H$ at the horizon crossing, i.e at $k = aH$. Thus, the full power spectrum of tensor perturbations, summing over the two polarization contributions, is given by

$$\mathcal{P}_t(k) = \frac{2\kappa^2}{\pi^2}H^2_\star. \tag{2.4.17}$$

If inflation was pure De Sitter, $H$ would be a constant and the spectrum would be the same for any mode $k$ leaving the horizon at different times. Instead, inflation generates a quasi-scale invariant spectrum. It acts as a quasi-De Sitter space in which $H$ is not exactly constant. Thus we have slight differences in the spectrum for modes leaving the horizon at different times;

modes leaving the horizon at earlier times will have a larger spectrum since $H$ shrinks.

For completeness, the power spectrum of scalar perturbations, is given by

$$\mathcal{P}_s(k) = \frac{\kappa^2}{8\pi^2}\frac{H^2}{\epsilon}\bigg|_{k=a}, \tag{2.4.18}$$

where $\epsilon$ is the slow-roll parameter defined in (2.3.10).

From these expression, one can obtain the scalar and tensor spectral indices defined in equations (2.4.6) and (2.4.8) in terms of slow-roll parameters in the slow-roll approximation,

$$n_s - 1 = 2\eta - 6\epsilon, \qquad n_t = -2\epsilon. \tag{2.4.19}$$

Scale invariance corresponds to $n_s = 1$ and $n_t = 0$. Since slow-roll condition imply $\eta, \epsilon \ll 1$, the expressions above show explicitly the nearly scale invariance of the power spectra. Moreover, define the *scalar-to-tensor* ratio as,

$$r \equiv \frac{\mathcal{P}_t}{\mathcal{P}_s} = 16\epsilon. \tag{2.4.20}$$

Measurements of these quantities strongly depend on the potential driving inflation. In fact, $H$ depends on the potential, $\epsilon$ and $\eta$ depend on the first and second derivative of the potential respectively. Therefore, the amplitude and the scale dependence of the perturbations encode information about the model driving inflation. Thus, they are an essential ingredient for our understanding of the early universe. Scalar perturbations have been deeply studied through CMB temperatures and polarization measure. Instead, tensor perturbations are much harder to detect.

Constraints on $n_s$ and $r$ are used to rule out or agree with inflationary models. The most reliable data we have up to date is that of the Planck observatory, which found the constraints $r < 0.11$ and $n_s = 0.9603 \pm 0.0073$ [25]. Recently, BICEP2 experiment on the South Pole detected inflationary gravitational waves in the B-mode of the power spectrum [26]. This predicted a value of the scalar-to-tensor ratio of $r = 0.2^{+0.07}_{-0.05}$. However, the contribution of foreground dust was not taken into account sufficiently and therefore their results may not be reliable.

# 3. Reheating

In the previous chapter, we reviewed the inflationary epoch and the behaviour and evolution of the inflaton $\phi$. If the Universe went through inflation, then it necessarily goes through a reheating process once inflation has ended. In fact, inflation ends once the inflaton leaves the slow-roll regime by rolling down to the minimum of the potential and starts oscillating.

In this section I will discuss the behaviour of the inflaton at the end of inflation and the following stages of reheating, i.e. preheating and thermalization, analytically. My discussion will focus on the chaotic inflationary model of a massless scalar inflaton field $\phi$ interacting with another scalar field $\chi$ with potential

$$V(\phi, \chi) = \frac{1}{4}\lambda\phi^4 + \frac{1}{2}g^2\phi^2\chi^2. \tag{3.0.1}$$

I will then analyse in detail the same process but in the case of non-minimal coupling between the two fields and gravity, presenting the possible values for the non-minimal coupling parameter. I will study analytically the evolution of the fields during preheating in the limit for small values of the non-minimal coupling and for large values of the inflaton.

I will then compute numerical lattice simulations on the behaviour of the fields during reheating for both the minimal and non-minimal coupling case using a modified version of the publicly available C++ LatticeEasy package [38]. This will allow me to observe the effects of the non-minimal coupling between matter and gravity during reheating.

## 3.1 Introduction: The two Stages of Reheating

The Universe starts reheating while the inflaton is oscillating around the minimum of the potential. The first phase of reheating is known as *preheating* and it is driven by parametric resonance between the inflaton field and the other scalar field $\chi$ [13]. The modes $\chi_k(t)$ are being amplified due to the resonance with $\phi$ and an exponentially fast production of $n_\chi$-particles is induced. This resonance is not influenced by the expansion of the Universe but depends sensitively and non-monotonically on the values of the parameters driving the resonance, such as the coupling parameters and the

initial conditions of the field. The resonance occurs within certain resonance bands which may strongly or weakly amplify the momentum modes of $\chi$. This results to be a very efficient stage of energy transfer between the two fields.

Parametric resonance can occur in two very different regimes; broad resonance and narrow resonance [13]. Narrow resonance occurs when the width of the resonance band is very small, as the name suggests. This usually implies a non-very effective resonance in which the modes are only slightly amplified. Moreover, the modes can very easily be shifted outside the resonance band and stop growing.

Broad resonance instead acts very differently to the narrow one and its dynamics is more complex. First of all, broad resonance is very efficient since the range of momenta which are amplified is significantly wide. The amplitude of the modes of the field $\chi$ will increase only when the inflaton field $\phi$ crosses zero during its oscillation. Meanwhile, for each inflaton oscillation, $\chi$ oscillates many times but the occupation number remains constant [13].

The nature of the resonance, broad or narrow, depends on the parameters setting the fields' evolution. Thus, it will strongly depend on the background inflationary model of the system. In any case, resonance ends once it becomes narrow and inefficient.

At this point, reheating enters its second stage of decay of produced particles. Here, it is important to remember to take into account the fields and particles that have been produced during the stage of preheating. The final stage of reheating involves a regime of semiclassical thermalization; the elementary particles that have been produced reach equilibrium and a thermalization temperature $T_r$ [15].

Unfortunately not much evidence can be carried out from this stage, making it very hard to make predictions on it. Furthermore, its behaviour is highly influenced by the preceding model of inflation so results from reheating would significantly help in understanding the inflationary regime too.

## 3.2 $\phi$ at the end of inflation

The evolution of the inflaton depends on the form of the potential driving inflation. In this section, I will be studying the evolution of $\phi$ with quartic potential $V = \lambda\phi^4$.

The slow-roll initial conditions imply that inflation lasts while $\phi > m_p$, where $m_p$ is the Planck mass [14]. In this phase, the dominant term (2.3.2) is the Hubble term. As the inflaton decreases, the Hubble term becomes less and less important until $\phi < m_p$, where inflation ends. At this stage, the inflaton rolls rapidly down the potential and starts oscillating around its minimum with initial amplitude $\Phi_0 \sim 0.1 m_p$ [14].

Consider the inflaton to be $\phi(t)$ satisfying,

$$\ddot{\phi} + 3H\dot{\phi} + \lambda\phi^3 = 0. \tag{3.2.1}$$

For convenience, we can rescale the field $\phi$ such that $\varphi = a\phi$. Rewriting the Klein-Gordon equation above in terms of $\varphi$ we obtain,

$$\varphi'' + \lambda\varphi^3 - \frac{a''}{a}\varphi = 0, \tag{3.2.2}$$

where $'$ indicates derivatives with respect to conformal time $\eta \equiv \int_0^t \frac{1}{a(t')}dt'$. This may be further simplified if one notices that after the end of inflation, the term $\frac{a''}{a}\varphi$ may be ignored. This is because in this theory, the stress energy tensor is traceless. This implies that $R = 0$, $a(\eta) \sim \eta$ and clearly $a'' = 0$. Thus we recover the equation of motion for a scalar field in Minkowski spacetime,

$$\varphi'' + \lambda\varphi^3 = 0. \tag{3.2.3}$$

One can explicitly show that the $\phi$-oscillations are not simply sinusoidal but given by elliptic functions. Again let's make use of a mathematical simplification by introducing a dimensionless conformal time variable $\tau \equiv \sqrt{\lambda}\varphi_i\eta$ where $\varphi_i$ is the amplitude of the field. Rescaling the function $\varphi = \varphi_i f(\tau)$, we find that it is a solution to (3.2.3) with,

$$f(\tau) = cn\left(\tau - \tau_o, \frac{1}{\sqrt{2}}\right). \tag{3.2.4}$$

The function $f(\tau)$ is the Jacobi elliptic cosine function [39]. It satisfies the relation $f'^2 = \frac{1}{2}\left(1 - f^4\right)$ and it is a periodic function with period $T \equiv 4K\left(1/\sqrt{2}\right) \approx 7.416$, where $K(m)$ is the complete elliptic integral of the first kind. The effective frequency of oscillation is therefore $2\pi/T \approx 0.8472$. A useful representation of the Jacobi elliptic cosine function is [39],

$$f(\tau) = \frac{8\pi\sqrt{2}}{T}\sum_{n=1}^{\infty}\frac{e^{-\pi(n-1/2)}}{1 + e^{-\pi(n-1/2)}}\cos\frac{2\pi\left(2n-1\right)\tau}{T}. \tag{3.2.5}$$

In this sum, the amplitude of the first oscillation is 0.9550. However, we notice that just after one oscillation, the amplitude of the field drops drastically to 0.04305 [14].

This elliptic cosine solution is a characteristic of $\phi^4$ theory. For quadratic potentials, the oscillations of $\phi$ at the start of reheating are simply sinusoidal. The fact that in $\phi^4$ theory they behave in this interesting manner will imply interesting results in the evolution of $\phi$ and $\chi$ in the following stages of reheating.

## 3.3 Preheating

Let me now find the equations governing the evolution of the fields during preheating. The evolution of $\chi$-fluctuations is governed by the Klein-Gordon equation in an expanding flat FRW Universe [14],

$$\ddot{\chi} + 3H\dot{\chi} - \frac{1}{a^2}\nabla^2\chi + V'(\phi, \chi) = 0, \tag{3.3.1}$$

where $H = \frac{\dot{a}}{a}$ and $\prime$ denotes the first derivative with respect to $\chi$ of the potential (3.0.1). Consider $\phi$ to be a classical scalar field interacting with a massless quantum field $\chi$. According to quantum field theory, we can expand $\chi$ in Fourier space in terms of creation and annihilation operators in this form,

$$\hat{\chi}(\mathbf{x}, t) = \frac{1}{(2\pi)^{3/2}} \int d^3k \left( \hat{a}_k \chi_k(t) e^{-i\mathbf{kx}} + \hat{a_k}^\dagger \chi_k^*(t) e^{-i\mathbf{kx}} \right). \tag{3.3.2}$$

Hence, the time-dependent part of $\chi$ satisfies the equation of motion,

$$\ddot{\chi_k} + 3H\chi_k + \left( \frac{k^2}{a^2} + g^2\phi^2 \right) \chi_k = 0. \tag{3.3.3}$$

Fluctuations of the $\phi$ field itself, $\phi_k$, are also present in this model due to the quartic term in the potential which leads to self-interactions of $\phi$ [13]. These satisfy a similar equation to (3.5.24) with a slight difference due to taking the derivative of the potential with respect to $\phi$ instead of $\chi$,

$$\ddot{\phi_k} + 3H\dot{\phi_k} + \left( \frac{k^2}{a^2} + 3\lambda\phi^2 \right) \phi_k = 0. \tag{3.3.4}$$

Since we have recovered the same form for the two equations of motion, we can work with $\chi$ fluctuations and apply similar results to $\phi$. Again for convenience, let's make use of conformal time $\eta$ defined in the previous section and conformal fields $\varphi$ and $X_k$ such that $\varphi = a(t)\phi$ and $X_k = a(t)\chi_k$. Applying this change of variables, (3.3.3) becomes

$$X_k'' + (k^2 + g^2\varphi^2)X_k = 0. \tag{3.3.5}$$

Now, in the same way as before, let's make use of the dimensionless conformal time $\tau \equiv \sqrt{\lambda}\varphi_i\eta$ and rewrite the equation in terms of derivatives of $\tau$ instead of $\eta$ by applying the chain rule to the equation. Moreover, using the solution of $\varphi$ derived in section 3.2, the equation above becomes,

$$X_k'' + \left( \kappa^2 + \frac{g^2}{\lambda} cn^2 \left( \tau, \frac{1}{\sqrt{2}} \right) \right) X_k = 0, \tag{3.3.6}$$

where $\kappa = \frac{k^2}{\lambda\varphi_i^2}$, $'$ corresponds to derivatives with respect to $\tau$ and I have dropped the initial value $\tau_0$ of the Jacobi cosine function.

The form of this expression is useful since we have removed any dependence on the expansion of the Universe and we have reduced the problem to one in Minkowski spacetime. This is only possible if the theory is conformally invariant. In this case, the potential only involves dimensionless parameters and hence they don't carry any physical length scale. This allows to map the model in an equivalent problem in Minkowski spacetime, which significantly simplifies the calculations.

Mathematically, equation (3.3.6) belongs to the family of Lamè equations [40]. It describes the oscillations of the field $X_k$ with frequency

$$w_k^2 = \kappa^2 + \frac{g^2}{\lambda} cn^2\left(\tau, \frac{1}{\sqrt{2}}\right). \tag{3.3.7}$$

Using the same steps, we find that similarly the oscillatory field $\varphi$ satisfies a Lamè equation of the form,

$$\varphi'' + \left(\kappa^2 + 3cn^2\left(\tau, \frac{1}{\sqrt{2}}\right)\right)\varphi = 0. \tag{3.3.8}$$

**Stability/Instability chart for the Lamè equation**

Equation (3.3.6) involves two parameters; the first one is $\kappa$, the momentum band and the second one is $g^2/\lambda$ which gives the strength of the resonance. Moreover, notice that its coefficients are periodic functions since, as mentioned before, the Jacobi elliptic cosine is in fact a periodic function. Differential equations with periodic coefficients such as the Lamè equation (3.3.6) are studied in Floquet theory [41]. According to Floquet's theorem, the Lamè equation admits solutions of the form,

$$X_k = f(\tau) exp[(\mu(k^2, g^2/\lambda))\tau], \tag{3.3.9}$$

where $\mu(k^2, g^2/\lambda)$ is the Floquet characteristic exponent which gives the strength of the resonance and $f(\tau)$ is a periodic function. The Floquet exponent is a function of the parameters $k^2$ and $g^2/\lambda$. When the Floquet exponent is complex, the solutions constitute stable-solutions. However, if it is real the solutions are no longer bounded and they are called unstable. Parametric resonance occurs only within instability bands, corresponding to real values of the Floquet exponent. Once $\mu_k$ is complex, $\chi$ simply oscillates and no resonance occurs [42]

The exponential growth of the modes $X_k$ implies an exponential growth in the occupation number $n_k$, such that,

$$n_k \sim |X_k|^2 \sim exp\left(2\mu_k\tau\right). \tag{3.3.10}$$

We expect fluctuations of $X$ to grow exponentially in specific bands of momentum $\kappa$ for some value of $g^2/\lambda$ as the inflaton field oscillates. What we're interested to find is for what values of the parameters the resonance is mostly amplified.

As we will see, the values of $g^2/\lambda$ will sensitively affect the strength of interaction between the two fields for specific bands of momentum in a non-trivial manner [14]. This is a very important point. If the fields underwent broad or narrow or stochastic resonance, the whole physics of the reheating process would change significantly. It would also affect, for instance, the production of gravitational waves during this era. Therefore, it is fundamental to discover the details of the parametric resonance and consequently, the behaviour of the fields.

The resonant modes for specific values of $g^2/\lambda$ was studied numerically in [14] by solving equation (3.3.6). The authors plotted a stability/instability chart of momentum modes against values of $g^2/\lambda$. It was found that the resonance bands stretch diagonally in the $(g^2/\lambda,\kappa^2)$ plane, implying some resonant structure for any value of $g^2/\lambda$ (see Figure 3.3.1).

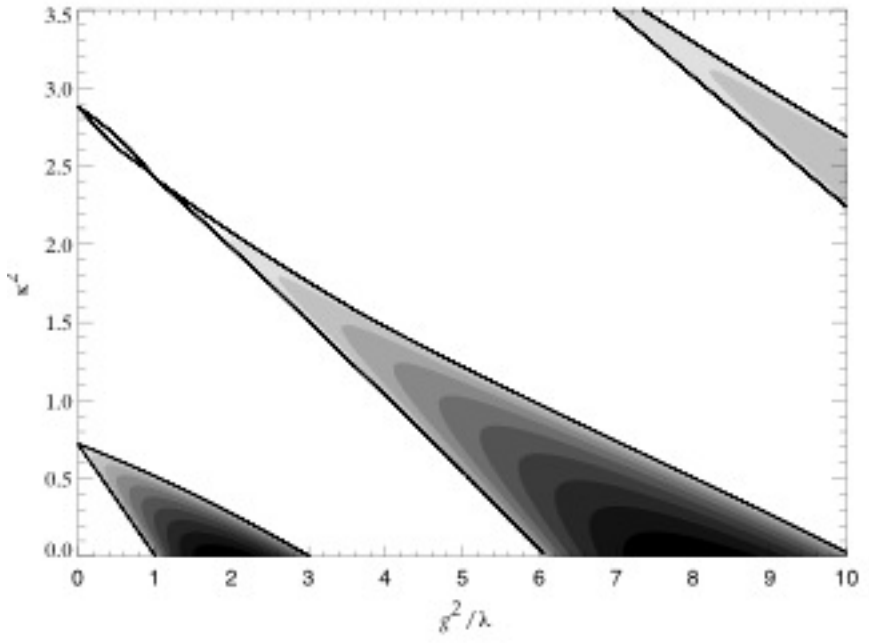


**Figure 3.3.1:** Stability/instability chart for the fluctuations $X_k$ obtained by solving numerically equation (3.3.6). Shaded(unshaded) areas are areas of instability(stability). The darker shade corresponds to a higher Floquet exponent. Figure taken by [14]

The shaded regions in figure 3.3.1 correspond to areas of instability in which the darker the shade, the higher is the Floquet exponent. The unshaded areas instead correspond to stable solutions. Therefore, parametric resonance

only occurs within shaded areas of figure 3.3.1. One can immediately notice that the largest characteristic exponent will occur for $\kappa^2 = 0$ between values $\frac{g^2}{\lambda} = \frac{n(n+1)}{2}$, with $n$ integer. For instance, $\kappa^2 = 0$ corresponds to the highest characteristic exponent for some value of $g^2/\lambda$ between $g^2/\lambda = 1$ and $g^2/\lambda = 3$ and between $g^2/\lambda = 6$ and $g^2/\lambda = 10$. A characteristic feature of the Lamè equation is that occasionally, some of the instability bands may shrink to a point. This implies that for instance for the values $g^2/\lambda = 1$ and $g^2/\lambda = 3$, there is a unique instability band.

More generally, there are a finite number of instability bands for $g^2/\lambda = \frac{n(n+1)}{2}$ and positive $\kappa^2$. However, all other values of $g^2/\lambda$ have an infinite number of instability bands. This a peculiar feature of this model, which differs very much from the quadratic model $V(\phi) = \frac{1}{2}m\phi^2$.

In the quadratic model, fluctuations obey the Mathieu equation instead of the Lamè equation [13]. Lamè equation's stability/instability chart results very similar to the Mathieu equation's one. The main difference is that its solutions have an infinite number of instability bands for each parameter q, analogous to our parameter $g^2/\lambda$. We will find that in the limit $g^2/\lambda \ll 1$, the Lamè equation may transform into a Mathieu equation of a particular form and the two stability/instability charts will coincide.

**Analytic Discussion of the Lamè Equation**

Earlier we found a solution to the Lamè equation in terms of transcendental Jacobi functions. Calculations involving these functions can be very complicated. Solutions to the Lamè equation for $\frac{g^2}{\lambda} = \frac{n(n+1)}{2}$ turn out to be simple, closed form solutions. Thus, I will focus on this case and rewrite the Lamè equation (3.3.6) in its algebraic form [14].

Let me introduce the time variable $z$ instead of $x$, such that,

$$z(x) = cn^2\left(x, \frac{1}{\sqrt{2}}\right), \qquad \text{and} \qquad \frac{d}{dx} = \sqrt{2z(1-z^2)}\frac{d}{dz}. \tag{3.3.11}$$

The equation for fluctuations $X_k$ then becomes,

$$2z(1-z^2)\frac{d^2X_k}{dz^2} + (1-3z^2)\frac{dX_k}{dz} + \left(\kappa^2 + \frac{g^2}{\lambda}z\right)X_k = 0. \tag{3.3.12}$$

Let $X_1(z)$ and $X_2(z)$ be two independent solutions of the equation above. One will be growing exponentially and the other will be decreasing exponentially. Now consider the three bilinear combinations $X_1^2$, $X_2^2$ and $X_1X_2$, which I will denote by $M(z)$, which obey a third equation, following from equation (3.3.12) [14],

$$2z\left(z^2-1\right)\frac{d^3M}{dz^3}+\left(9z^2-3\right)\frac{d^2M}{dz^2}-2\left[\left(2\frac{g^2}{\lambda}-3\right)z+2\kappa^2\right]\frac{dM}{dz}-2\frac{g^2}{\lambda}M=0. \tag{3.3.13}$$

Restricting to solutions for values of $\frac{g^2}{\lambda}=\frac{n(n+1)}{2}$, the solutions are of polynomial form of degree n.

For the purposes of this thesis, I will analyse in full details the interesting case $g^2/\lambda=1$. The solution to (3.3.13) is $M_1(z)=z-2\kappa^2$ [14]. Here, $M_1(z)$ is clearly the product of an exponential growing function and an exponential decreasing one, i.e $M_1(z)=X_1(z)X_2(z)$. Thus, we recover the expression,

$$X_1(z)X_2(z)=z-2\kappa^2. \tag{3.3.14}$$

Furthermore, I will be using the notion of the Wronskian of a function [43]. The Wronskian of a set of n-1 times differentiable functions $f_1,..,f_n$ over an interval is defined as the determinant of the square matrix constructed by placing the functions in the first row, the first derivatives on the second row, and so on til the (n-1) derivative. In our cause, from equation (3.3.12), we can easily recover the Wronskian for X(z),

$$W(X_1,X_2)\equiv X_1\frac{dX_2}{dz}-X_2\frac{dX_1}{dz}=\frac{A}{\sqrt{z(1-z^2)}}, \tag{3.3.15}$$

where A is some constant. The two equations (3.3.14) and (3.3.15) form two simultaneous equations from which one can recover the closed form solutions,

$$X_{1,2}(z)=\sqrt{|M_1(z)|}exp\left(\pm\frac{A}{2}\int\frac{dz}{\sqrt{z(1-z^2)}M_1(z)}\right). \tag{3.3.16}$$

The constant A can be found by substituting this solution back into (3.3.12), from which one finds $A=\sqrt{2\kappa^2(1-4\kappa^4)}$. Recall that the two solutions describe one an exponentially growing function and one an exponentially decreasing one. For the exponentially growing one, one must set the constraint for A to be real. As a result, the growing solutions (for $\kappa^2>0$) occur in the range $0<\kappa^2<\frac{1}{2}$. Moreover, we have discussed that the growing solution must be of the form $X(x)=P[z(x)]e^{\mu_k x}$. Thus, using (3.3.16), one can find the Floquet exponent $\mu_k$ as a function of $\kappa$ for $g^2/\lambda=1$. Therefore, the Floquet exponent is [14],

$$\mu_k(\kappa)=\frac{2}{T}\sqrt{2\kappa^2(1-4\kappa^4)}\int_0^{\pi/2}d\theta\frac{sin^{1/2}\theta}{1+2\kappa^2 sin\theta}, \tag{3.3.17}$$

where T is the period of oscillations, $T\approx 7.416$. The maximum value for the characteristic exponent for the case $g^2/\lambda=1$ is $\mu_{max}\approx 0.1470$ at $\kappa^2\approx 0.228$, in agreement with Figure 3.3.1.

Similarly, the same procedure can be applied for the $\phi$-oscillations, corresponding to the case $g^2/\lambda = 3$, for which it is found that$\mu_{max} \approx 0.03598$ at $\kappa^2 = 1.615$. In Greene's *et al.* paper [14], solutions for the two cases $g^2/\lambda \ll 1$ and $g^2/\lambda \gg 1$ are also widely explained. Here, I will only state its main results.

As mentioned before, in the limit $g^2/\lambda \ll 1$, the equation for $X_k(x)$ becomes the Mathieu equation,

$$\frac{d^2X_k}{d\tau^2} + (A + 2qcos2\tau)X_k = 0, \tag{3.3.18}$$

where $\tau = \frac{2\pi x}{T}$, $A = \left(\frac{T_k}{2\pi}\right)^2$ and $q = 0.4570 \times \frac{g^2}{2\lambda}\left(\frac{T}{2\pi}\right)^2$. Thus, in this limit, the parametric resonance corresponds to that described by the Mathieu equation. It predicts narrow instability bands around $\kappa^2 = \frac{2\pi m}{T}$ with $m = 1, 2, ..$ and a maximum characteristic exponent of the exponentially growing solution $X_k \propto e^{\mu_k x}$ with value $\mu_{max} \approx 0.1467 \times \frac{g^2}{\lambda}$. In conclusion, in this regime the parametric resonance is that of narrow resonance with very small resonance bands width.

In the limit $g^2/\lambda \gg 1$, the system behaves like in broad resonance regime. Firstly, we observe that the evolution of the modes $X_k$ is adiabatic. Moreover, the number density of particles $n_k(x)$ changes only when at $x = x_j$ the inflaton's amplitude crosses zero, i.e. when $\phi(x = x_j) = 0$, and is constant otherwise. Thus, one can simply consider the evolution of $X_k$ where $\phi^2$ is small and it is $\propto (x - x_j)^2$, resembling a quadratic potential. Then, one can combine the effects of all subsequent parabolic potentials to find the overall particle creation number. Using this method, one finds that in this limit the Lamè equation can be reduced to the simpler form,

$$\frac{d^2X_k}{dx^2} + \left(\kappa^2 + \frac{g^2}{2\lambda}(x - x_j)^2\right)X_k = 0. \tag{3.3.19}$$

The resonance in this regime will be efficient for $\kappa^2 \leq \sqrt{\frac{g^2}{2\pi^2\lambda}}$. It was found that for a given value of $g^2/\lambda$, there will be a sequence of stability/instability bands as a function of $\kappa$ and the width of the instability bands where the resonance is efficient is $\Delta\kappa^2 \simeq \sqrt{\frac{g^2}{2\lambda}}$. Like in the other cases, the characteristic exponent results to be a non-monotonic function of $g^2/\lambda$. However, an interesting result is that for $g^2/\lambda \to \infty$, the function $\mu_{max}(g^2/\lambda)$ approaches asymptotically the value 0.2377. Thus, we find that in this regime the resonance is stronger both in terms of the characteristic exponent $\mu_{max}$ and the width $\kappa^2$.

In conclusion, we have proved that the $\chi$-particle production depends non-monotonically on $g^2/\lambda$. It is less efficient for $g^2 \ll \lambda$ than in all other regimes. Furthermore, the $\chi$-particle production is generally more efficient than the production of $\phi$-particles, except for regimes where $\chi$-particle production

is inefficient. An interesting point is that the particles which are mostly produced during reheating are those with the greatest characteristic exponent $\mu$ and not those most strongly coupled to the inflaton, as one may naively think.

## 3.4 Thermalization

When does the resonance end? Since the theory is a conformally invariant theory, we showed that it is possible to eliminate the scale factor from the equations governing the system. Hence, the expansion of the Universe doesn't affect the resonance structure, nor the end of the resonance. The only effect which determines the end of the resonance in this theory is the backreaction of created particles which restructures the resonance band [13]. When the resonance band is very narrow, this occurs at $\langle\varphi^2\rangle \ll \varphi^2$. All it is needed is a small shift in the position of the resonance band in momentum space. In this way, resonance modes which were growing will not grow anymore.

Preheating is only the first stage of reheating and it doesn't lead to a complete decay of the inflaton. During the second stage of reheating, created particles interact with each other and the inflaton field until semiclassical equilibrium is reached. It is believed that the last stages of the inflaton decay occur in a perturbative regime, opposite to the non-perturbative regime of preheating. After this perturbative regime, the decay products have energies higher than the thermal energy and number density lower than the thermal number density [15]. Thus, thermalization occur once interactions are at equilibrium. It is shown that the process of decay is the dominant interaction leading to thermalization. The study of thermalization is important in order to estimate the reheating temperature and the possibility of out-of-equilibrium states [44].

## 3.5 Non-minimal coupling to gravity

So far, I have considered reheating in a chaotic inflationary model involving two interacting scalar fields. Many chaotic inflationary models have been modified and extended over the years. Extensions are made in order to explore the effects of adding certain terms to a certain system. These additions may provide more accurate models or, as importantly, discard others. This approach consists of adding terms which act as sources, to the Einstein-Hilbert action..

I chose to study a model which contains in addition an interaction term between gravity and matter. This model has not been studied before in the cases I will be discussing in this thesis and I hope it will provide further help in the probe of a unique inflationary theory.

It was realised before that there is nothing preventing interactions between matter and gravity. In General Relativity, gravity is a consequence of the geometry of spacetime. Therefore, interactions between gravity and matter are described by an interaction term involving the fields (matter part) and the Ricci scalar (gravitational part), which I chose to be of the form $\xi\phi^2 R + \xi\chi^2 R$.

Cosmologists have been studying inflationary models containing this kind of interaction term in the action for theories such as Higgs inflation and pure $\lambda\phi^4$ theory [45], [46], [47]. In addition, since the coupling $\xi$ is dimensionless, it is a marginal operator and hence it corresponds to a renormalisable term. According to renormalisation theory, this suggests that such a term should be included in the action.

As mentioned in the introduction, an interaction term of the form $\xi R\phi^2$ is called a non-minimal coupling term. In general, it is called a non-minimal coupling term if it differs from the standard Einstein-Hilbert term of the form $\sqrt{-g}R/\kappa^2$. Therefore, minimal coupling corresponds to $\xi = 0$. Actions including non-minimally coupled terms are said to be in the Jordan Frame. On the other hand, an action in the Einstein frame is one including only minimally coupled terms. However, an action in the Jordan frame can be rewritten in the Einstein frame via a conformal transformation [48]. A conformal transformation consists essentially of variable and field redefinitions and therefore the two frames are mathematically equivalent. This equivalence should also appear for any physical quantity in the two frames [46].

In this section, I will analyse how the addition of this type of term will affect the dynamics of reheating both analytically and numerically. I chose the non-minimal coupling parameter, $\xi$, to be the same for both fields. This was my particular choice, but there is nothing preventing the two fields from having different non-minimal coupling.

The action of this system in the Jordan frame is,

$$S = \int d^4x\sqrt{-g}\left(\frac{1}{2\kappa^2}R - \frac{1}{2}\partial_\mu\phi\partial^\mu\phi - \frac{1}{2}\partial_\mu\chi\partial^\mu\chi - \frac{1}{2}\xi R\phi^2 - \frac{1}{2}\xi R\chi^2 - V(\phi,\chi)\right), \tag{3.5.1}$$

where $g = det(g_{\mu\nu})$, $\phi$ and $\chi$ are light scalar fields, R is the Ricci scalar, $\kappa^2 = 8\pi G$, $\xi$ is the coupling between the scalar fields and curvature and $V(\phi,\chi) = \frac{1}{4}\lambda\phi^4 + \frac{1}{2}g^2\phi^2\chi^2$.

The inflaton field $\phi$ and $\chi$ obey respectively the following Klein-Gordon equations,

$$\begin{aligned} \Box\phi - \xi R\phi + \frac{dV}{d\phi} &= 0, \\ \Box\chi - \xi R\chi + \frac{dV}{d\chi} &= 0, \end{aligned} \tag{3.5.2}$$

where the terms $\xi R\phi$ and $\xi R\chi$ describe the explicit interaction between the fields and the curvature, i.e. between the matter and gravitational sector.

### 3.5.1 Values of $\xi$

Originally, Futamase and Maeda [45] added a non-minimal coupling term to the action since it seemed to alleviate the fine tuning problem of the self coupling constant $\lambda$ in $\phi^4$ potential.

For chaotic inflation with quartic potential, $V(\phi) = \lambda\phi^4$ minimally coupled to gravity ($\xi = 0$), $\lambda \sim 10^{-14}$ which is smaller than the expected natural value of a coupling in particle physics. This is known as the fine-tuning problem of the coupling $\lambda$ in this theory. This is one of the main reasons why $\phi^4$ theory was ruled out of possible inflationary models. Adding the non-minimal coupling between the inflaton and gravity, partially solves this problem since the constraint on $\lambda$ is relaxed by several orders of magnitude.

Fakir and Unruh proposed a strong nonminimal coupling, $\xi > 1$ [49]; since the coupling $\xi$ is essentially free, if one takes $\xi = O(10^4)$ then the correct amplitude of density perturbations can be achieved with $\lambda = (10^{-1})$. This is because in this model, the amplitude of density perturbations will depend on the ratio $\frac{\lambda}{\xi^2}$ instead of $\lambda$. Hence, choosing an appropriate value for $\xi$ allows any value of $\lambda$ desired. This was originally what brought cosmologists to investigate the effects of non-minimal coupling to gravity.

There are many reasons why we should expect an interacting term between gravity and matter. First of all, when describing the evolution of an interacting quantum scalar field in spacetime with large curvature, such a term arises naturally. This leads to the so called *$\xi$-problem* [50]: Should physics imply a unique value of $\xi$?

There are some specific values of $\xi$ which arise quite naturally and which seems to suggest that not only the non minimal coupling is unavoidable but also that $\xi$ is not a free parameter. The value of $\xi$ must depend on the theory of gravity and on the properties of the scalar field $\phi$.

It was proven that if gravity is described by a metric theory and $\phi$ has non-gravitational origin, then $\xi$ takes the value $\xi = 1/6$ [51]. This specific case is called of *conformal coupling*. This result arises by imposing the Einstein Equivalence Principle(EEP) on the physics of the field $\phi$. The Einstein Equivalence principle is an extension of the Weak Equivalence Principle(WEP); it states that WEP holds and that the outcome of any local non-gravitational test experiment is independent of the velocity of the freely falling apparatus (Local Lorentz Invariance, LLI) and of where and when in the universe it is performed (Local Position Invariance, LPI). According to this, calculations show that $\xi$ must take the value $1/6$. If not, we would allow a massive field to propagate along the light cone, which we know it is only possible for massless objects.

If this is the case, the whole perception of inflation in this theory must be

revisited. In fact, so far we have treated $\xi$ as a free parameter which we could freely choose in order to alleviate the fine tuning problem of $\lambda$. However, if $\xi = 1/6$ is the value of the parameter *a priori*, then we need to find out if inflation is still a possible scenario of the early Universe. Moreover, if inflation is possible, what are the consequences of this induced inflationary scenario.

Futamase and Maeda [45] found out that actually inflation is not possible at all in $\phi^4$ theory if the inflaton is conformally coupled to gravity. This was quite straightforward to prove. The potential $V(\phi) = \lambda\phi^4$ is conformally invariant due to the parameter being scale invariant. Consequently, the whole system is scale invariant and the trace of the energy-momentum tensor vanishes. Therefore, the Einstein equations yield

$$\dot{H} - 2H^2 + \frac{k^2}{a} = 0. \tag{3.5.3}$$

Solving this equation, we find that for $k = 0$, $a \propto t^{1/2}$ and for $k = -1$, $a \propto t$ asymptotically. Neither of these are inflationary solutions since during inflation $a$ evolves quasi-exponentially. This means that according to this theory, inflation doesn't take place at all. In conclusion, chaotic inflation cannot exist in a quartic potential theory conformally coupled to gravity.

In my discussion, I will consider cases of both weak and strong coupling. According to observational constraints, the most reliable data is given by the Planck observatory's 2013 results, which found $\xi < -0.0019$ for $\lambda\phi^4$ theory [25]. Thus, we can rule out the possibility of $\xi > 0$ and concentrate on values of $\xi$ which agree with Planck's constraint.

### 3.5.2 From the Jordan frame to the Einstein frame

In order to study the behaviour of the system, both analytically and numerically, it is easier to conformally transform the action to the Einstein frame. In this way, we will recover an action without the non-minimal coupling term and its dependence will be incorporated in the potential. Therefore all the information on the evolution of the system can be found by studying the behaviour of the potential only. The new action will be mathematically equivalent to the original one but it will have removed the non-minimally coupled term, making calculations simpler. A conformal transformation is a change of coordinates, such that the metric changes by [48],

$$\tilde{g}_{\mu\nu}(x) = \Omega^2 g_{\mu\nu}(x). \tag{3.5.4}$$

Consequently, the inverse metric will transform as $\tilde{g}^{\mu\nu}(x) = \Omega^{-2} g^{\mu\nu}(x)$ and its determinant as $\sqrt{-\tilde{g}} = \Omega^4\sqrt{-g}$. The Ricci scalar R arises from the contraction of the metric to the Ricci tensor, i.e. $R = g_{\mu\nu}R^{\mu\nu}$, and hence it will also be affected by the transformed metric. In fact the conformally

transformed Ricci scalar, in 4 dimensions, takes the form [48],

$$\tilde{R} = \frac{1}{\Omega^2}\left(R - \frac{6}{\Omega}\Box\Omega\right), \tag{3.5.5}$$

where $\Box = g^{\mu\nu}\nabla_\mu\nabla_\nu\Omega$. Rewriting the action (3.5.1) in terms of the transformed metric $\tilde{g}^{\mu\nu}(x)$ and Ricci scalar $\tilde{R}$, we obtain the action,

$$\begin{aligned} S = \int d^4x \frac{\sqrt{-\tilde{g}}}{\Omega^4}\Bigg[\frac{1}{2\kappa^2}\left(\Omega^2\tilde{R} + \frac{6}{\Omega}\Box\Omega\right) - \frac{1}{2}\tilde{g}^{\mu\nu}\Omega^2(\partial_\mu\phi\partial_\nu\phi + \partial_\mu\chi\partial_\nu\chi) - \\ - \frac{1}{2}\xi\left(\phi^2+\chi^2\right)\left(\Omega^2\tilde{R} + \frac{6}{\Omega}\Box\Omega\right) - V(\phi,\chi)\Bigg] \end{aligned} \tag{3.5.6}$$

$$\begin{aligned} = \int d^4x\sqrt{-\tilde{g}}\Bigg[\frac{1}{2}\left(\frac{1-\kappa^2\xi(\phi^2+\chi^2)}{\kappa^2\Omega^2}\right)\tilde{R} + 3\left(\frac{1-\kappa^2\xi(\phi^2+\chi^2)}{\kappa^2\Omega^5}\right)\Box\Omega \\ -\frac{1}{2}\frac{\tilde{g}^{\mu\nu}}{\Omega^2}(\partial_\mu\phi\partial_\nu\phi + \partial_\mu\chi\partial_\nu\chi) - \frac{V(\phi,\chi)}{\Omega^4}\Bigg]. \end{aligned} \tag{3.5.7}$$

It is easy to see that the appropriate transformation in order for the first term to be in the Einstein-Hilbert form, $\sqrt{-g}R/2\kappa^2$, is $\Omega^2 = 1 - \kappa^2\xi(\phi^2+\chi^2)$. Furthermore, the second term of (3.5.7) can be absorbed by a rescaling of the fields $\phi$ and $\chi$. We introduce the rescaled fields $\tilde{\phi}(\phi,\chi)$ and $\tilde{\chi}(\phi,\chi)$ such that,

$$\frac{1}{2}\left(\tilde{\partial}_\mu\tilde{\phi}\tilde{\partial}^\mu\tilde{\phi} + \tilde{\partial}_\mu\tilde{\chi}\tilde{\partial}^\mu\tilde{\chi}\right) = \frac{1}{2\Omega^2}\left(\tilde{\partial}_\mu\phi\tilde{\partial}^\mu\phi + \tilde{\partial}_\mu\chi\tilde{\partial}^\mu\chi\right) + 3\left(\frac{1-\kappa^2\xi\left(\phi^2+\chi^2\right)}{\kappa^2\Omega^5}\right)\Box\Omega. \tag{3.5.8}$$

In principle, one should also include a cross term of the form $\partial_\mu\tilde{\phi}\partial^\mu\tilde{\chi}$ in the LHS of equation (3.5.8) since $\tilde{\phi}$ and $\tilde{\chi}$ are functions of both $\phi$ and $\chi$ and would therefore generate the cross term. By including such a term, we would recover non-separable and not canonically normalizable kinetic terms due to their coefficient being mixed functions of both $\phi$ and $\chi$. In order to make the calculations simpler, I will restrict my interest to canonically normalizable fields and therefore ignore the cross term.

Let me expand the term involving $\Box\Omega$ in a simpler form. Consider,

$$\int d^4x \left( \frac{1-\kappa^2\xi\left(\phi^2+\chi^2\right)}{\Omega^5} \right) \Box\Omega \tag{3.5.9}$$

$$= \int d^4x \frac{\Box\Omega}{\Omega^3}, \tag{3.5.10}$$

$$= \int d^4x \frac{\Omega g^{\mu\nu}\nabla_\mu\nabla_\nu\Omega}{\Omega^4}, \tag{3.5.11}$$

$$= \int d^4x \frac{1}{\Omega^4}\left[-g^{\mu\nu}\nabla_\mu\Omega\nabla_\nu\Omega + g^{\mu\nu}\nabla_\mu\left(\Omega\nabla_\nu\Omega\right)\right], \tag{3.5.12}$$

$$= -\int d^4x \frac{1}{\Omega^4}\left[g^{\mu\nu}\nabla_\mu\left(1-\kappa^2\xi(\phi^2+\chi^2)\right)^{1/2}\nabla_\nu\left(1-\kappa^2\xi(\phi^2+\chi^2)\right)^{1/2}\right], \tag{3.5.13}$$

$$= -\int d^4x \frac{\kappa^4\xi^2}{\Omega^6}\left(\phi^2(\partial\phi)^2+\chi^2(\partial\chi)^2\right), \tag{3.5.14}$$

where in the third line I have integrated by parts and assumed that the term $g^{\mu\nu}\nabla_\mu\left(\Omega\nabla_\nu\Omega\right)$ vanishes.

Thus, using the result of equation (3.5.14), equation (3.5.8) can be rewritten in the simpler form,

$$\frac{1}{2}\tilde{\partial}_\mu\tilde{\phi}\tilde{\partial}^\mu\tilde{\phi}+\frac{1}{2}\tilde{\partial}_\mu\tilde{\chi}\tilde{\partial}^\mu\tilde{\chi} = \frac{1}{2\Omega^2}\left(\tilde{\partial}_\mu\phi\tilde{\partial}^\mu\phi+\tilde{\partial}_\mu\chi\tilde{\partial}^\mu\chi\right)+\frac{3\kappa^2\xi^2}{\Omega^4}\left(\phi^2\tilde{\partial}_\mu\phi\tilde{\partial}^\mu\phi+\chi^2\tilde{\partial}_\mu\chi\tilde{\partial}^\mu\chi\right). \tag{3.5.15}$$

Since both $\tilde{\phi}$ and $\tilde{\chi}$ are both functions of $\phi$ and $\chi$, using the chain rule we have,

$$\partial_\mu\tilde{\phi} = \frac{\partial\tilde{\phi}}{\partial\phi}\partial_\mu\phi+\frac{\partial\tilde{\phi}}{\partial\chi}\partial_\mu\chi, \tag{3.5.16}$$

$$\partial_\mu\tilde{\chi} = \frac{\partial\tilde{\chi}}{\partial\phi}\partial_\mu\phi+\frac{\partial\tilde{\chi}}{\partial\chi}\partial_\mu\chi. \tag{3.5.17}$$

Using these expressions for $\partial_\mu\tilde{\phi}$ and $\partial_\mu\tilde{\chi}$ one can expand the LHS of equation (3.5.15), to obtain,

$$\frac{1}{2}\left[\left(\frac{\partial\tilde{\phi}}{\partial\phi}\right)^2+\left(\frac{\partial\tilde{\chi}}{\partial\phi}\right)^2\right]\tilde{\partial}_\mu\phi\tilde{\partial}^\mu\phi+\left[\left(\frac{\partial\tilde{\phi}}{\partial\phi}\right)\left(\frac{\partial\tilde{\phi}}{\partial\chi}\right)+\left(\frac{\partial\tilde{\chi}}{\partial\phi}\right)\left(\frac{\partial\tilde{\chi}}{\partial\chi}\right)\right]\tilde{\partial}_\mu\chi\tilde{\partial}^\mu\phi$$
$$+\frac{1}{2}\left[\left(\frac{\partial\tilde{\phi}}{\partial\chi}\right)^2+\left(\frac{\partial\tilde{\chi}}{\partial\chi}\right)^2\right]\tilde{\partial}_\mu\chi\tilde{\partial}^\mu\chi = \frac{\Omega^2+6\kappa^2\xi^2\phi^2}{2\Omega^4}\tilde{\partial}_\mu\phi\tilde{\partial}^\mu\phi+\frac{\Omega^2+6\kappa^2\xi^2\chi^2}{2\Omega^4}\tilde{\partial}_\mu\chi\tilde{\partial}^\mu\chi. \tag{3.5.18}$$

By equating coefficients in the equation above, we obtain the following relations between the rescaled fields and the old fields,

$$\begin{aligned}
\left(\frac{\partial\tilde{\phi}}{\partial\phi}\right)^2 + \left(\frac{\partial\tilde{\chi}}{\partial\phi}\right)^2 &= \frac{\Omega^2 + 6\kappa^2\xi^2\phi^2}{\Omega^4}, \\
\left(\frac{\partial\tilde{\phi}}{\partial\chi}\right)^2 + \left(\frac{\partial\tilde{\chi}}{\partial\chi}\right)^2 &= \frac{\Omega^2 + 6\kappa^2\xi^2\chi^2}{\Omega^4}, \\
\left(\frac{\partial\tilde{\phi}}{\partial\phi}\right)\left(\frac{\partial\tilde{\phi}}{\partial\chi}\right) + \left(\frac{\partial\tilde{\chi}}{\partial\phi}\right)\left(\frac{\partial\tilde{\chi}}{\partial\chi}\right) &= 0.
\end{aligned} \tag{3.5.19}$$

This system of PDEs does not have an exact solution for $\tilde{\phi}(\phi, \chi)$ and $\tilde{\chi}(\phi, \chi)$. I have tried to simplify and solve this system analytically in many ways but each time it would lead to a system of contradictory equations. I have tried solving this on Mathematica, which also could not solve it. Moreover, I tried by writing the fields in terms of polar coordinates, i.e. $\phi = \rho\sin\theta$ and $\chi = \rho\cos\theta$, in order for the non-minimal coupling term in the action (3.5.1) to be a function of just $\rho$, but this also did not lead to any solvable system. We can therefore conclude that an exact rescaling under these assumptions is not possible and I will need to make a further approximation. The reason could be that I have neglected the possibility of a non-zero cross term between $\partial_\mu\tilde{\phi}$ and $\partial_\mu\tilde{\chi}$ in the LHS of equation (3.5.8). Moreover, the prolem is that we are trying to reduce it to a problem in flat FLRW spacetime by ignoring its curvature. However, a rotation that allows us to do this cannot be done and hence we find that an exact solution to the system does not exist.

Most of the literature which encounters this same problem simplifies the system by assuming $\Omega$ to be a function of only $\phi$ and rescales $\chi$ such that $\tilde{\chi} = \chi$ [52]. However, in this way, the system is reduced to a model in which only the inflaton results to be non-minimally coupled to gravity. In order to take into account interactions of both the fields with gravity, I chose a different approximation, such that,

$$\frac{\partial\tilde{\chi}}{\partial\phi} = \frac{\partial\tilde{\phi}}{\partial\chi} \ll 1, \tag{3.5.20}$$

in order to have $\tilde{\phi}$ being dominated by $\phi$ and $\tilde{\chi}$ being dominated by $\chi$. By making this assumption, the system (3.5.19) reduces to,

$$\left(\frac{\tilde{\partial}\tilde{\phi}}{\tilde{\partial}\phi}\right)^2 = \frac{\Omega^2 + 6\kappa^2\xi^2\phi^2}{\Omega^4} \qquad \text{and} \qquad \left(\frac{\tilde{\partial}\tilde{\chi}}{\tilde{\partial}\chi}\right)^2 = \frac{\Omega^2 + 6\kappa^2\xi^2\chi^2}{\Omega^4} \quad . \tag{3.5.21}$$

Due to the the way we have constructed the fields $\tilde{\phi}$ and $\tilde{\chi}$, i.e. by equation (3.5.8), the action (3.5.7) in terms of the rescaled fields $\tilde{\phi}$ and $\tilde{\chi}$ takes the form,

$$S_E = \int d^4x\sqrt{-\tilde{g}}\left(-\frac{1}{2\kappa^2}\tilde{R} + \frac{1}{2}\tilde{\partial}_\mu\tilde{\phi}\tilde{\partial}^\mu\tilde{\phi} + \frac{1}{2}\tilde{\partial}_\mu\tilde{\chi}\tilde{\partial}^\mu\tilde{\chi} - \tilde{V}(\tilde{\phi},\tilde{\chi})\right). \quad (3.5.22)$$

where $\tilde{\partial}_\mu\tilde{\partial}^\mu = \tilde{g}^{\mu\nu}\partial_\mu\partial_\nu$. The potential in the Einstein frame takes the form,

$$\tilde{V}(\tilde{\phi},\tilde{\chi}) = \frac{1}{(1-\kappa^2\xi(\phi^2+\chi^2))^2}\left[\frac{1}{4}\lambda\phi^4 + \frac{1}{2}g^2\phi^2\chi^2\right]. \quad (3.5.23)$$

The action (3.5.22) is clearly in the Einstein frame since it is given by a gravitational part, which takes the Einstein-Hilbert form $\sqrt{-g}R/\kappa^2$, and a matter sector. We notice that the potential is non-renormalizable, as a potential in 4 dimensions with terms of higher power than 4 are non-renormalizable. It therefore seems to be unphysical and one may think that something went wrong. However, this argument is irrelevant for our purposes since we are using this form of the action only to be able to study the system in the simplest form possible. We in fact know that the physical action we are describing is the original one in the Jordan frame which is a renormalisable theory. Hence, we can interpret the conformal transformation to the action (3.5.22) as a mathematical tool in order to study the system in a more convenient frame. The action (3.5.22) yields the following equations of motion for $\phi$ and $\chi$ (after relabelling $\tilde{\phi}$ to $\phi$ ,$\tilde{\chi}$ to $\chi$, etc.),

$$\begin{aligned}\ddot{\phi} + 3\frac{\dot{a}}{a}\dot{\phi} - \frac{1}{a^2}\nabla^2\phi + \frac{\partial V}{\partial\phi} = 0,\\ \ddot{\chi} + 3\frac{\dot{a}}{a}\dot{\chi} - \frac{1}{a^2}\nabla^2\chi + \frac{\partial V}{\partial\chi} = 0.\end{aligned} \quad (3.5.24)$$

Clearly, the explicit non-minimal coupling term in equations (3.5.2) has disappeared. This is because it is implicitly part of the term involving the derivative of the potential. This is the reason why it is easier to study a system in the Einstein frame; its evolution is determined by its potential only. However, the potential in equation (3.5.23) is still in terms of the old fields $\phi$ and $\chi$. In order to find its explicit dependence on $R$ we must rewrite it in terms of the rescaled fields $\tilde{\phi}$ and $\tilde{\chi}$ or equivalently, in its Einstein frame form. In order to do this, the first step is to solve equations (3.5.21) and find the explicit form of $\phi$ and $\chi$ in terms of $\tilde{\phi}$ and $\tilde{\chi}$. Using those expression, one can then rewrite the potential in the Einstein form.

Solving (3.5.21) exactly is rather complicated. An easier way to deal with this is to again make use of approximations. This will allow me to deal

with simpler forms of the potential which are valid within specific ranges of either $\xi$ or $\phi$, according to the choice of approximation. I chose to take the limit for small value of $\xi$, small values of the inflaton field $\phi$ and large values of the field $\phi$. I will then focus on computing numerical simulations in the small $\xi$ approximation which will hopefully be able to reveal the effect of the non-minimal coupling term on the reheating process.

### 3.5.3 Small $\xi$ approximation

Let me first consider the small $\xi$ regime. In this limit, I can Taylor expand the expressions in powers of $\xi$. By Taylor expanding (3.5.21) about $\xi = 0$ up to first order in $\xi$, I obtain,

$$\begin{aligned}\frac{\partial\tilde{\phi}}{\partial\phi} &= \left(\frac{\Omega^2 + 6\kappa^2\xi^2\phi^2}{\Omega^4}\right)^{1/2}, \\ &= \frac{\left(1 - \kappa^2\xi(\phi^2+\chi^2) + 6\kappa^2\xi^2\phi^2\right)^{1/2}}{1 - \kappa^2\xi(\phi^2+\chi^2)}, \\ &\simeq 1 + \frac{1}{2}\kappa^2\xi(\phi^2+\chi^2) + O(\xi^2).\end{aligned} \tag{3.5.25}$$

Similarly for $\tilde{\chi}$,

$$\begin{aligned}\frac{\partial\tilde{\chi}}{\partial\chi} &= \left(\frac{\Omega^2 + 6\kappa^2\xi^2\chi^2}{\Omega^4}\right)^{1/2}, \\ &= \frac{\left(1 - \kappa^2\xi(\phi^2+\chi^2) + 6\kappa^2\xi^2\chi^2\right)^{1/2}}{1 - \kappa^2\xi(\phi^2+\chi^2)}, \\ &\simeq 1 + \frac{1}{2}\kappa^2\xi(\phi^2+\chi^2) + O(\xi^2).\end{aligned} \tag{3.5.26}$$

Since we are assuming $\partial\tilde{\phi}/\partial\chi$ and $\partial\tilde{\chi}/\partial\phi$ to be negligible, equations (3.5.25) and (3.5.26) can be integrated to obtain,

$$\begin{aligned}\tilde{\phi} &\simeq \phi + \frac{1}{2}\xi\kappa^2\chi^2\phi + \frac{1}{6}\xi\kappa^2\phi^3 + O(\xi^2), \\ \tilde{\chi} &\simeq \chi + \frac{1}{2}\xi\kappa^2\phi^2\chi + \frac{1}{6}\xi\kappa^2\chi^3 + O(\xi^2),\end{aligned} \tag{3.5.27}$$

Notice that these expressions are consistent with the assumption made in equation (3.5.20). We have that $\frac{\partial\tilde{\phi}}{\partial\chi} = \frac{\partial\tilde{\chi}}{\partial\phi} \approx \kappa^2\xi\chi\phi$. We know that initially this definitely holds since we have $\chi_0 = 0$ and $\xi$ is always very small. Moreover, at later times, $\phi$ also decreases and $\chi$ never increases too much to make this assumption invalid.

Recall that what we need in order to write the potential in the Einstein form is an expression for $\phi(\tilde{\phi},\tilde{\chi})$ and $\chi(\tilde{\phi},\tilde{\chi})$. Thus we need to invert equations (3.5.27). One can do this by writing $\phi$ and $\chi$ as an expansion in terms of powers of $\xi$ up to order $\xi^2$, i.e.

$$\phi(\tilde{\phi},\tilde{\chi}) = A + \xi B + O(\xi^2), \qquad \chi(\tilde{\phi},\tilde{\chi}) = C + \xi D + O(\xi^2). \tag{3.5.28}$$

By substituting this in equations (3.5.27), one can easily recover expressions for the coefficients $A$,$B$,$C$,$D$ by equating coefficients of similar terms on the LHS and RHS of the equation. In particular, we find,

$$\begin{aligned}
\phi(\tilde{\phi},\tilde{\chi}) &\simeq \tilde{\phi} - \xi\left(\frac{1}{2}\kappa^2\tilde{\chi}^2\tilde{\phi} + \frac{1}{6}\kappa^2\tilde{\phi}^3\right) + O(\xi^2),\\
\chi(\tilde{\phi},\tilde{\chi}) &\simeq \tilde{\chi} - \xi\left(\frac{1}{2}\kappa^2\tilde{\phi}^2\tilde{\chi} + \frac{1}{6}\kappa^2\tilde{\chi}^3\right) + O(\xi^2).
\end{aligned} \tag{3.5.29}$$

The potential in the Einstein frame takes the form,

$$\begin{aligned}
\tilde{V}(\tilde{\phi},\tilde{\chi}) &= \frac{1}{\Omega^4}V[\phi(\tilde{\phi},\tilde{\chi}),\chi(\tilde{\phi},\tilde{\chi})],\\
&= \frac{1}{\left(1-\kappa^2\xi(\phi^2+\chi^2)\right)^2}\left[\frac{1}{4}\lambda\phi^4 + \frac{1}{2}g^2\phi^2\chi^2\right],\\
&\simeq \left(1+2\kappa^2\xi(\phi^2+\chi^2)\right)\left(\frac{1}{4}\lambda\phi^4 + \frac{1}{2}g^2\phi^2\chi^2\right) + O(\xi^2),\\
&\simeq \frac{1}{4}\lambda\phi^4 + \frac{1}{2}g^2\phi^2\chi^2 + \xi\left[\frac{1}{2}\kappa^2\phi^6 + \left(\frac{1}{2}\lambda + g^2\right)\kappa^2\chi^2\phi^4 + g^2\kappa^2\phi^2\chi^4\right] + O(\xi^2),\\
&\simeq \frac{1}{4}\lambda\tilde{\phi}^4 + \frac{1}{2}g^2\tilde{\phi}^2\tilde{\chi}^2 + \frac{1}{3}\xi\left[g^2\kappa^2\tilde{\chi}^2\tilde{\phi}^4 + g^2\kappa^2\tilde{\chi}^4\tilde{\phi}^2 + \lambda\kappa^2\tilde{\phi}^6\right] + O(\xi^2),
\end{aligned} \tag{3.5.30}$$

where in the last line I have used the expressions for $\phi$ and $\chi$ in equation (3.5.29). Again the above form of $\tilde{V}$ is the approximation of the effective potential in the limit for small $\xi$. It is taken up to first order in $\xi$ since it would not add any information to take it up to any further order once we've taken all other expressions up to first order in $\xi$. From this expression, it is now trivial to obtain the form of the derivatives of $\tilde{V}$ with respect to $\tilde{\phi}$ and $\tilde{\chi}$ needed to solve the equations of motion (3.5.24),

$$\begin{aligned}
\frac{\partial\tilde{V}}{\partial\tilde{\phi}} &\simeq \lambda\tilde{\phi}^3 + g^2\tilde{\phi}\tilde{\chi}^2 + \xi\left[\frac{2}{3}\kappa^2 g^2\tilde{\phi}\tilde{\chi}^4 + \frac{4}{3}g^2\kappa^2\tilde{\phi}^3\tilde{\chi}^2 + 2\lambda\kappa^2\tilde{\phi}^5\right] + O(\xi^2)\\
\frac{\partial\tilde{V}}{\partial\tilde{\chi}} &\simeq g^2\tilde{\phi}^2\tilde{\chi} + \xi\left[\frac{2}{3}\kappa^2 g^2\tilde{\phi}^4\tilde{\chi} + \frac{4}{3}\kappa^2 g^2\tilde{\phi}^2\tilde{\chi}^3\right] + O(\xi^2)
\end{aligned} \tag{3.5.31}$$

**Small $\phi$ approximation**

Here I apply the same procedure I used for the small $\xi$ approximation. This time, instead of Taylor expanding about $\xi = 0$, I Taylor expanded the expressions (3.5.21) about $\phi = 0$. As before, I obtained an expression for the derivative of $\tilde{\phi}$ with respect to $\phi$ in polynomial form, which is easily integrable. Furthermore, rearranging I finally found an expression for $\phi$ in terms of $\tilde{\phi}$.

Here, I noticed that the result I obtained was exactly the same I recovered from approximating in the small $\xi$ regime. This is a very interesting point. This means that the system obeys the same equations of motion and therefore has the same behaviour in the limit for small $\xi$ and in the limit for small $\phi$. However, in principle, the two approximations are very different. In the former, one recovers a potential valid for *all* values of the fields if their non-minimal coupling to gravity is relatively small. In the latter, one recovers a potential which can describe the evolution of the small fields with any value of the non-minimal coupling parameter. It is an interesting point which I will further explain when dealing with numerical simulations.

### 3.5.4 Large $\phi$ approximation

In the large $\phi$ approximation, the procedure I adopted is slightly different. In this regime, the two fields $\phi$ and $\chi$ behave very differently. This is because we take the inflaton to be large but the same approximation is not possible for the field $\chi$. In fact, $\chi$ is necessarily light and small at the end of inflation. Thus, we need to find a different way to treat $\chi$. Especially in this regime, since we are considering the inflaton to be large, it is clear that the dominant term of the potential will be that including the inflaton.

Consequently, the effect of the non-minimal coupling between gravity and matter will be prevalently from the coupling with the inflaton. The effect of the non-minimal coupling between gravity and $\chi$ will be smaller and can therefore be neglected in this approximation.

In order to do this, consider the action describing the system in the Jordan frame (3.5.1) and let the two fields $\phi$ and $\chi$ have different non-minimal couplings $\xi$ and $\zeta$ respectively. Now impose $\zeta = 0$ so that $\chi$ is minimally coupled to gravity. Thus, the action (3.5.1) becomes,

$$S = \int d^4x\sqrt{-g}\left(\frac{1}{2\kappa^2}R - \frac{1}{2}\partial_\mu\phi\partial^\mu\phi - \frac{1}{2}\partial_\mu\chi\partial^\mu\chi - \frac{1}{2}\xi R\phi^2 - V(\phi,\chi)\right). \tag{3.5.32}$$

Now, as I did before, I will rewrite the action in the Einstein frame using conformal transformations. The steps are the same as when both the fields were non-minimally coupled to gravity. However, the situation here is even simpler. This time, the metric transforms as

$$\tilde{g}_{\mu\nu} = \Omega^2 g_{\mu\nu}, \quad \text{with} \quad \Omega^2 = 1 - \xi\kappa^2\phi^2. \tag{3.5.33}$$

.

By rewriting the action in terms of the conformally transformed metric and Ricci scalar ( see section 3.5.2 for details on the Ricci scalar transformation), one obtains

$$S = \int d^4x\sqrt{-g}\left[\frac{1}{2\kappa^2}\tilde{R} - \frac{3}{\kappa^2}\left(\frac{\kappa^4\xi^2\phi^2(\tilde{\partial}\phi)^2}{\Omega^6}\right) - \frac{1}{2\Omega^2}\left(\tilde{\partial}_\mu\phi\tilde{\partial}^\mu\phi + \tilde{\partial}_\mu\chi\tilde{\partial}^\mu\chi\right) - \frac{1}{\Omega^4}V(\phi,\chi)\right]. \tag{3.5.34}$$

This action is clearly in the Einstein frame but it is useful to further rewrite it in the standard form of equation (3.5.22). To do this, introduce new fields $\tilde{\phi}$ and $\tilde{\chi}$ such that the second term in the equation above disappears. Again, I will make the assumption,

$$\frac{\partial\tilde{\chi}}{\partial\phi} = \frac{\partial\tilde{\phi}}{\partial\chi} \ll 1. \tag{3.5.35}$$

In this way I can absorb the second term in equation (3.5.34) by defining the rescaled fields $\tilde{\phi}$ and $\tilde{\chi}$ such that,

$$\frac{1}{2}\tilde{\partial}_\mu\tilde{\phi}\tilde{\partial}^\mu\tilde{\phi} = \frac{1}{2\Omega^2}\tilde{\partial}_\mu\phi\tilde{\partial}^\mu\phi + 3\frac{\kappa^2\xi^2\phi^2}{\Omega^4}(\tilde{\partial}\phi)^2, \quad \Longrightarrow \left(\frac{\partial\tilde{\phi}}{\partial\phi}\right)^2 = \frac{\Omega^2 + 6\kappa^2\xi^2\phi^2}{\Omega^4}, \tag{3.5.36}$$

$$\frac{1}{2}\tilde{\partial}_\mu\tilde{\chi}\tilde{\partial}^\mu\tilde{\chi} = \frac{1}{2\Omega^2}\tilde{\partial}_\mu\chi\tilde{\partial}^\mu\chi, \qquad \Longrightarrow \left(\frac{\partial\tilde{\chi}}{\partial\chi}\right)^2 = \frac{1}{\Omega^2}. \tag{3.5.37}$$

Since $\Omega$ is a function of $\phi$ only and ignoring $\partial\tilde{\chi}/\partial\phi$ by assumption, equation (3.5.37) can be integrated to recover,

$$\chi \simeq (1 - \kappa^2\xi\phi^2)^{1/2}\tilde{\chi}. \tag{3.5.38}$$

Again, under the assumption that $\partial\tilde{\phi}/\partial\chi$ is small enough to be neglected, I have integrated (3.5.36) using Mathematica to recover the exact solution,

$$\kappa\sqrt{-\xi}\tilde{\phi} = \sqrt{1-6\xi}\sinh^{-1}\left(\sqrt{1-6\xi}\kappa\sqrt{-\xi}\phi\right) - \sqrt{-6\xi}\sinh^{-1}\left(\sqrt{-6\xi}\frac{\kappa\sqrt{-\xi}\phi}{\sqrt{1-\kappa^2\xi\phi^2}}\right). \tag{3.5.39}$$

This expression seems rather complicated. However, recall that we are interested in the limit for large $\phi$. More rigorously, the limit I am considering is that of $\tilde{\phi} \gg \frac{M_p}{\xi}$. Thus, I can approximate $\sqrt{1-6\xi} \approx \sqrt{-6\xi}$ and use the

relation $\sinh^{-1} x = \ln\left(x + \sqrt{x^2+1}\right)$, valid for any value of $x$. Using this, my expression simplifies as,

$$\kappa\sqrt{-\xi}\tilde{\phi} \approx \frac{\sqrt{-6\xi}}{2}\ln\left(1-\kappa^2\xi\phi^2\right)^{1/2} \implies \Omega^2 = \exp\left(\sqrt{\frac{2}{3}}\kappa\tilde{\phi}\right). \tag{3.5.40}$$

Using $\Omega^2 = 1 - \xi\kappa^2\phi^2$, we can rearrange the above expression in order to find $\phi$ in terms of the new field $\tilde{\phi}$. One obtains,

$$\phi^2 = \frac{1}{\kappa^2\xi}\left(1 - \exp\left(\sqrt{\frac{2}{3}}\kappa\tilde{\phi}\right)\right). \tag{3.5.41}$$

Using equation (3.5.41) and (3.5.38) we can find an explicit expression for the potential $\tilde{V}(\tilde{\phi},\tilde{\chi})$ in terms of the new fields $\tilde{\phi}$ and $\tilde{\chi}$ as we did for the small $\xi$ approximation. The potential in the Einstein frame for large values of $\phi$ is,

$$\begin{aligned}
\tilde{V}(\tilde{\phi},\tilde{\chi}) &= \frac{1}{\Omega^4}V[\phi(\tilde{\phi},\tilde{\chi}),\chi(\tilde{\phi},\tilde{\chi})], \\
&= \exp\left(2\sqrt{\frac{2}{3}}\kappa\tilde{\phi}\right)\left(\frac{\lambda}{4}\phi^4 + \frac{1}{2}g^2\phi^2\chi^2\right), \\
&\simeq \frac{\lambda}{4\kappa^4\xi^2}\left(1 - e^{-\sqrt{2/3}\kappa\tilde{\phi}}\right)^2 - \frac{g^2}{2\kappa^2\xi}\left(1 - e^{-\sqrt{2/3}\kappa\tilde{\phi}}\right)\tilde{\chi}^2.
\end{aligned} \tag{3.5.42}$$

where in the last line I have used the expressions for $\phi(\tilde{\phi},\tilde{\chi})$ and $\chi(\tilde{\phi},\tilde{\chi})$ of equations (3.5.38) and (3.5.41). From now on I will relabel any quantity $\tilde{X}$ to $X$. Recall that in order to solve the equations of motion for $\chi$ and $\phi$ we will need the derivatives of the potential with respect to $\phi$ and $\chi$. These can be easily deduced from the approximate form of the potential above,

$$\frac{dV}{d\phi} = \frac{\alpha}{2\kappa\xi}\left(\frac{\lambda}{\kappa^2\xi} - g^2\chi^2\right)e^{-\alpha\kappa\phi} - \frac{\alpha\lambda}{2\kappa^3\xi^2}e^{-2\alpha\kappa\phi}, \tag{3.5.43}$$

$$\frac{dV}{d\chi} = \frac{g^2}{\kappa^2\xi}\left(e^{-\alpha\kappa\phi} - 1\right)\chi, \tag{3.5.44}$$

where $\alpha = \sqrt{2/3}$.

I found that in the large $\phi$ approximation of my model, one can notice a strong correlation with the Higgs-inflationary model [53].

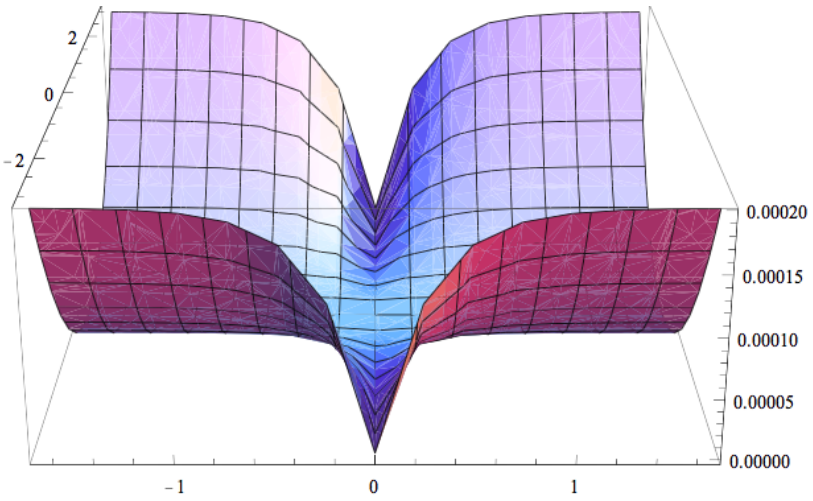


**Figure 3.5.1:** Graph of the potential in the large $\phi$ approximation

## 3.6 Numerical Simulations

The dynamics during preheating is highly non-linear and non-homogenous. For this reason, we must solve the equations of motion of the fields numerically. I used LatticeEasy, a C++ public program made available by Gary Felder and Igor Tkachev [38]. In this section I will firstly give an overview on the functioning of the program which will be mainly based on the available online documentation [38].

LatticeEasy runs lattice simulations of the evolution of interacting scalar fields in an expanding Universe. It is easily applicable to any inflationary model with multiple interacting fields. More specifically, the main equations that the program solves are the equations of motion of the scalar fields and that of the evolution of the scale factor, i.e.

$$\begin{aligned} \ddot{f} + 3\frac{\dot{a}}{a}\dot{f} - \frac{1}{a^2}\nabla^2 f + \frac{\partial V}{\partial f} = 0, \\ \ddot{a} + 2\frac{\dot{a}^2}{a} - \frac{8\pi}{a}\left(\frac{1}{3} \mid \nabla f_i \mid^2 + a^2 V\right) = 0. \end{aligned} \tag{3.6.1}$$

The program uses a staggered leapfrog algorithm to solve such equations. It stores the values of the variables (and its first derivative) at each time step and from those, it computes the value of the second derivative. It will compute this process at each fixed time step, each time overwriting the old values.

One important point is that the program variables are not the physical variables. Firstly because it would be very hard to create a simulation able

to deal with very small variables, as for instance $\lambda$ which is of order $10^{-13}$. Furthermore, rescalings make the equations simpler and hence the simulations quicker. It is therefore important to remember that any result obtained by the simulations will be in terms of the rescaled variables and not the physical variables.

The variable rescalings can be written in the general form,

$$f_{pr} \equiv Aa^r f; \quad x_{pr} \equiv Bx; \quad dt_{pr} \equiv Ba^s dt. \tag{3.6.2}$$

The rescaling variables $A$,$B$,$r$ and $s$ are chosen depending on what is most useful for a particular model. However, the LatticeEasy documentation provides guidelines in setting these variables. The first is that it is useful to rescale in order to eliminate the derivative term from the equations of motion. The second is that it is convenient to set the scale of the field variables to be of order unity at least initially. From these two conditions, it follows immediately that,

$$s - 2r + 3 = 0, \quad \text{and} \quad A = \frac{1}{\phi_0}, \tag{3.6.3}$$

where $\phi_0$ is the initial value fo the inflaton. Furthermore, the calculations are simplified if the rescalings imply that the coefficient of the dominant potential term to be of order unity and to include no powers of the scale factor.

Assuming the dominant term of the potential is of the form $V = \frac{cpl}{\beta}\phi^\beta$ and putting all these conditions together, we have the relations,

$$A = \frac{1}{\phi_0}; \quad B = \sqrt{cpl}\phi_0^{-1+\beta/2}; \quad r = \frac{6}{2+\beta}; \quad s = 3\frac{2-\beta}{2+\beta}. \tag{3.6.4}$$

Thus, if one simply sets $\beta$,$cpl$ and $\phi_0$ then all other variables will be automatically set by (3.6.4). For my particular potential, my choice of rescaling was the same made by G.Felder and I.Tkachev in their default model, i.e. $cpl = \lambda$ and $\beta = 4$. This implies that the fields are rescaled such that, $\phi_{pr} = \frac{a}{\phi_0}\phi$ and $\chi_{pr} = \frac{a}{\phi_0}\phi$ and the rescaled potential is $V_{pr} = \frac{a^4}{\lambda\phi_0^4}V$.

Another important aspect of the simulations is choosing the appropriate lattice parameters. The choice of the parameters that describe the lattice very much depend on the physical features of the model. Two of the most important parameters are the lattice size L and the number of points on the lattice, N. Firstly, one must make sure that the volume of the lattice $L^3$ doesn't exceed the Hubble horizon. This assures that approximating spacetime as a flat FLRW spacetime is a valid assumption. Moreover, it is important to make sure that the grid spacing $L/N$ covers all typical wavelengths of the fluctuations.

For my model, I chose $\lambda = 9 \times 10^{-14}$, in agreement with WMAP data [7]. The initial value of $a$ is set to 1 and the initial value of the inflaton $\phi_0$

is set to be $\phi_0 = 0.342 M_{pl}^2$ such that initially $\dot{\phi_0} = -H_\star \phi_0$, where $H_\star$ is the Hubble constant at the end of inflation, $H_\star^2 \simeq 2.6^{-15} M_{pl}^2$. The initial value of $\chi_i$ is more complex to choose. It sets the initial background of $\chi$, which is different for each Hubble volume since at the end of inflation the value of $\chi$ varies on superhorizon scales due to its lightness. Thus, any quantity which depends on $\chi_i$ will also vary between different horizon volumes. As I will explain in more detail later, the amplitude of gravitational waves produced during reheating, $\Omega_{GW}$, is a function of $\chi_i$ and it is therefore highly sensitive to the choice of $\chi_i$ [54]. However, it is not the purpose of this thesis to study the sensitivity of the system on the choice of $\chi_i$. Therefore, for computational convenience, I will choose the initial value of $\chi$ to be $\chi_i = 0$.

LatticeEasy generates several outputs; Once it has calculated the evolution of the fields, it also calculates many functions involving different physical quantities about the fields. For instance, it calculates the means and variances of all output fields. The means are the sum of the field at each gridpoint divided by the total number of gripoints. The variance is given by $Variance(f) = \langle f^2 \rangle - \langle f \rangle^2$.

Another important quantity which the program calculates is the spectra of all the fields. Within the spectra, most importantly it provides the occupation number $n_k$ and the energy spectrum $\rho_k$. The occupation number $n_k$ is an adiabatic invariant of the field evolution and its integral $n \sim \int d^3k n_k$ is the classical number density (in the large amplitude limit). Mathematically, it is given by

$$n_k \equiv \frac{1}{2}\left( w_k |\tilde{F}_{k,c}|^2 + \frac{1}{w_k} |\tilde{F}'_{k,c}|^2 \right), \tag{3.6.5}$$

where $w_k$ is the frequency of the oscillation and $\tilde{F}_{k,c}$ is a modified Fourier transform of the field $f$ in terms of conformal variables, such that $\tilde{F}_k = 1/L^{3/2} F_k$. Conformal variables are needed in order to take into account the expansion of the Universe. As for the energy spectrum $\rho_k$, it shows the energy spectrum of the field in different Fourier modes and it is given by,

$$\rho_k \equiv w_k n_k = \frac{1}{2}\left( w_k^2 |\tilde{F}_{k,c}|^2 + |\tilde{F}'_{k,c}|^2 \right). \tag{3.6.6}$$

The default inflationary model considered in G.Felder and I.Tkachev's program is that of chaotic inflation with a $\lambda\phi^4$ inflaton potential and another massless light scalar field coupled to the inflaton. The potential is of the form,

$$V = \frac{1}{4}\lambda\phi^4 + \frac{1}{2} g^2 \phi^2 \chi^2. \tag{3.6.7}$$

I modified the LatticeEasy code in order to study the inflationary model I am interested in, i.e. that of an inflaton and another scalar field coupled to gravity, and compared it to the default model. This allowed me to analyse in

detail what the effect of the non-minimal coupling term is on reheating and later on, on the production of gravitational waves.

In this section, I will firstly compute lattice simulations and present the results for the minimally coupled model with the potential (3.6.7). Then, I will study the non-minimally coupled system with the same potential and conclude on the effect of the non-minimally coupling term.

### 3.6.1 Minimal coupling case

First of all, let me analyse the behaviour of the fields during reheating with the potential $V = \frac{1}{4}\lambda\phi^4 + \frac{1}{2}g^2\phi^2\chi^2$ for a system minimally coupled to gravity, i.e. $\xi = 0$.

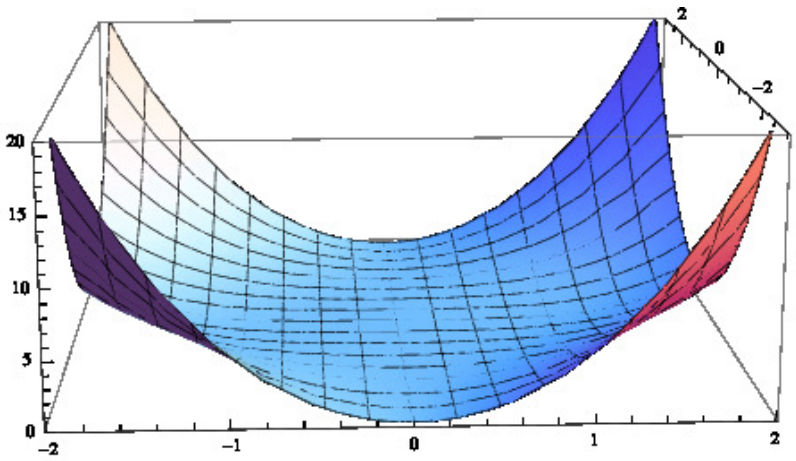


**Figure 3.6.1:** Graph of the rescaled potential $V = \frac{1}{4}\phi^4 + \frac{1}{2}\frac{g^2}{\lambda}\phi^2\chi^2$.

As mentioned above, this is the default model used by I.Tkachev and G.Felder in LatticeEasy. In the previous sections, we studied the system analytically up to its non-linear behaviour. A numerical analysis is necessary in order to study the dynamics of its non-linear nature.

For the numerical simulations, I chose the coupling's value to be $g^2/\lambda = 1$. As discussed, the initial values of the fields are $\phi_0 = 0.342M_{pl}^2$ and $\chi_0 = 0$, which assures its lightness at the start of reheating. As for the parameters which specify the lattice, I made several runs in order to find the appropriate lattice volume $V = L^3$ and number of lattice points, $N$. I found that the choice N=64 and L=80 made sure that the lattice spacing included all relevant modes amplified during the simulation.

Figures 3.6.2 and 3.6.3 show the evolution of the mean amplitude squared $a^2\phi^2$ and $a^2\chi^2$. Recall that the functions that are being plotted are those rescaled into program variables. Therefore, time $t$ on the x-axis is actually the rescaled conformal time, such that $dt_{\rm pr} = \left(\sqrt{\lambda}\phi_0/a\right)dt$. These figures are useful to describe the early times of preheating since it reproduces the

evolution of the 0-mode. Initially, the inflaton is much larger than that of $\chi$ and it oscillates with varying amplitude til $t \sim 120$.

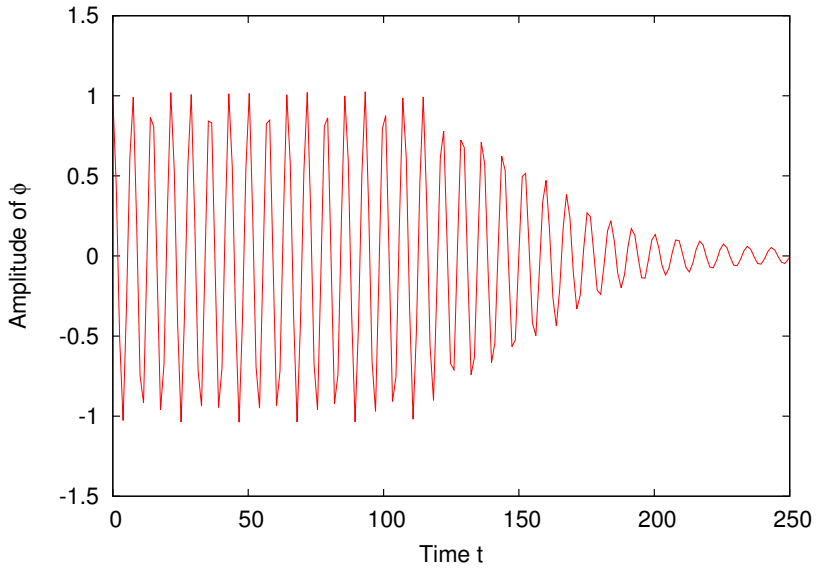


**Figure 3.6.2:** Mean amplitude squared of the inflaton $a^2\phi^2$.

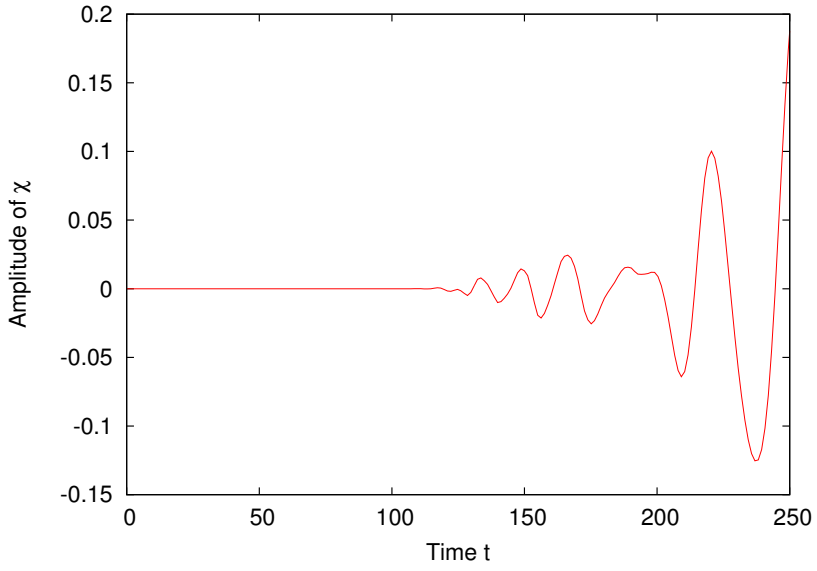


**Figure 3.6.3:** Mean amplitude squared of $a^2\chi^2$.

These oscillations induce a resonant exponential growth in the fluctuations $\chi$. This can be clearly appreciated from figure 3.6.4. It shows the evolution of the variances of $\phi$ and $\chi$ and it is more useful to describe later times of

preheating since it includes all modes' evolution. One can notice that the variance in $\phi$ also increases due to its self coupling and interactions with $\chi$ but only at $t \sim 150$ when $\chi$ has already been amplified significantly.

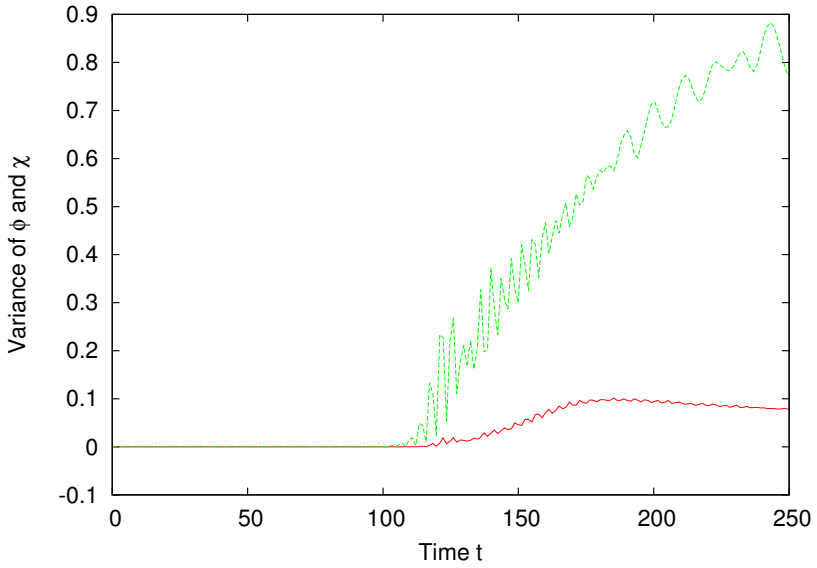


**Figure 3.6.4:** Evolution of the variances $a^2\left(\langle\phi^2\rangle - \langle\phi\rangle^2\right)$ and $a^2\left(\langle\phi^2\rangle - \langle\phi\rangle^2\right)$. The fields are in units of $\phi_0$ and $t$ is the rescaled program time.

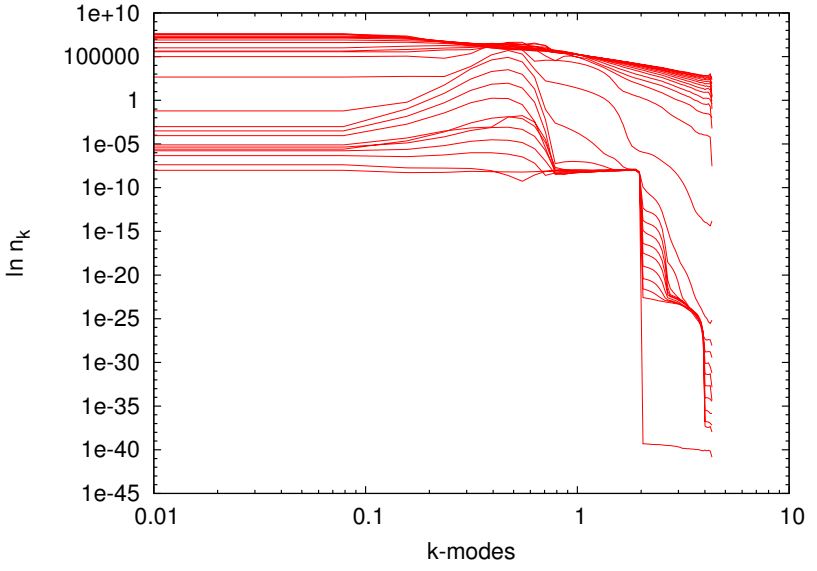


**Figure 3.6.5:** Occupation number $n_\chi$ opposed to momentum modes in logarithmic scale

The exponential growth of $\chi$ arising from the parametric resonance with

$\phi$ also implies an increase in the $\chi$-particles occupation number. This can be clearly seen in figure 3.6.5. The modes which are being amplified during the parametric resonance are those which induce the number occupation of $\chi$-particles to grow by many orders of magnitude.

Moreover, from figures 3.6.2 and 3.6.3 one can see that eventually they will reach the same amplitude due to the energy transfer from $\phi$ to $\chi$ and the resonance will terminate.

### 3.6.2 Non-minimal coupling case

Firstly, notice that the form of the equations of motion that the program is built to solve (equation (3.6.1)) coincides with the form of the equations of motion recovered by conformally transforming the action from the Jordan frame to the Einstein frame(equations (3.5.24). Hence, LatticeEasy runs simulations on the evolution of the fields in the Einstein frame. The potential and its first derivative are the functions which encode all the information needed to solve the scale factor equation and the fields equations of motion. In this section, I will present numerical simulations made in the regime of small values of the coupling $\xi$.

**Small $\xi$ regime**

Recall that in section 3.4.1, under the assumption of small $\xi$, I derived the following expressions for the potential, (and from that, expressions for its derivatives with respect to $\phi$ and $\chi$),

$$\tilde{V}(\tilde{\phi},\tilde{\chi}) \simeq \frac{1}{4}\lambda\tilde{\phi}^4 + \frac{1}{2}g^2\tilde{\phi}^2\tilde{\chi}^2 + \frac{1}{3}\xi\left[g^2\kappa^2\tilde{\chi}^2\tilde{\phi}^4 + g^2\kappa^2\tilde{\chi}^4\tilde{\phi}^2 + \lambda\kappa^2\tilde{\phi}^6\right] + O(\xi^2) \tag{3.6.8}$$

This must be rescaled into program variables in order to be able to run the code. As discussed, my choice of rescalings are $\phi_{pr} = \frac{a}{\phi_0}\phi$ and $\chi_{pr} = \frac{a}{\phi_0}\chi$ and the rescaled potential is $V_{pr} = \frac{a^4}{\lambda\phi_0^4}V$. For convenience, I also defined a new parameter $\xi_{pr}$, such that $\xi_{pr} = \xi\phi_0^2$. Again, we will need to take into account these rescalings when drawing conclusions on the outputs of the program.

Figure 3.6.6 is the plot of the (rescaled) potential of equation (3.6.8). Here, I have chosen the particular value $\xi = -0.002$, just about in agreement with the CMB according to Planck's data.

One can notice that the plot shows that the potential drops at a certain value of the inflaton. By plotting the potential with many different values of $\xi$, I found that this happens for any choice of $\xi$ within Planck's constraint. Thus, although the potential was constructed to be valid for small values of $\xi$ and all values of the inflaton, the potential is only applicable within a certain range of $\phi$. Once this limit is surpassed, the potential drops and any simulation fails to run.

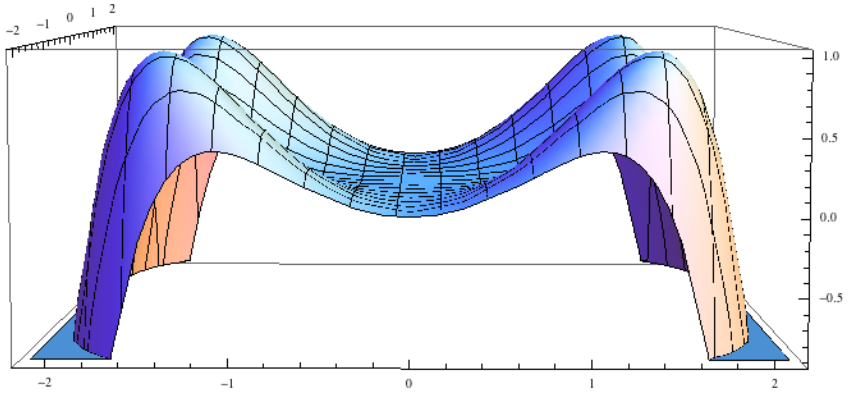


**Figure 3.6.6:** Graph of the rescaled potential (3.5.23) with $\xi = -0.002$

Moreover, by performing various runs of the code and studying the behaviour of the system in the different cases, I concluded that my approximation is only valid for values $\xi$ such that $\xi \geq -0.2$. Hence, I restricted my analysis of the system in this approximation to values of $\xi$ within the range $-0.2 \leq \xi < -0.0019$.

The simulations in this regime carried out interesting results. We found that the behaviour of the fields in the case of non-minimal coupling to gravity very similar to that in the minimal coupling case.

The mean amplitude squared of the inflaton field $\phi$ and the scalar field $\chi$ are plotted in figure 3.6.7 and 3.6.8. As before, we see that the inflaton is initially larger than $\chi$ and that it undergoes an oscillatory phase. In the same way as in the minimal coupled case, these oscillations induce an exponential growth in the fluctuations of $\chi$ which can be clearly seen in figure 3.6.9.

The strong amplification of $\chi$-modes also induces a rapid increase on the number of occupation $n_k$, and hence on the production of $\chi$-particles as one can see from figure 3.6.10. It is interesting to notice that the values of the modes which are being amplified via parametric resonance are the same for both minimal and non-minimal coupling regimes.

If we compare very carefully these graphs to the corresponding ones in the minimally coupled scenario then we can spot some slight difference. For instance, the oscillations of $\phi$ at early times are greater than those in the minimally coupled case and it seems to be decaying to a larger amplitude at later times. However, the overall physical dynamics of the two systems shows essentially the same behaviour.

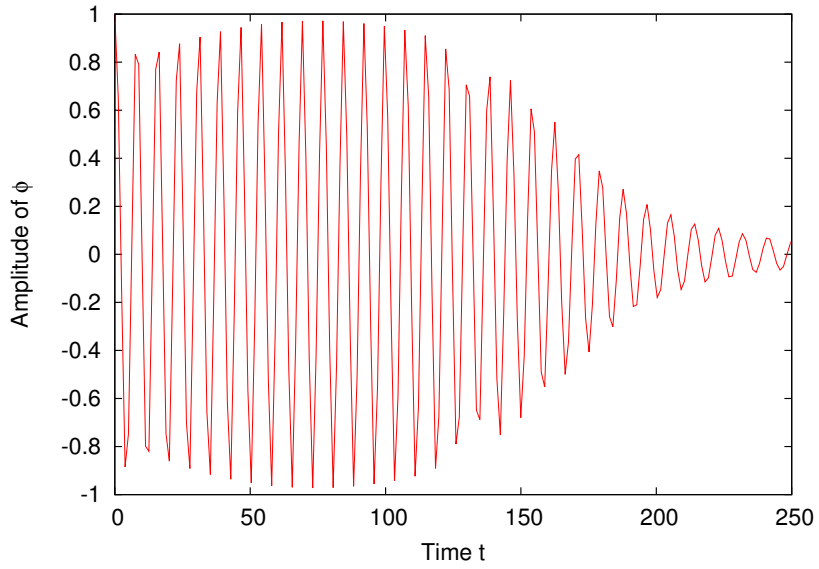


**Figure 3.6.7:** Mean amplitude of $\phi$ in small $\xi$ approximation.

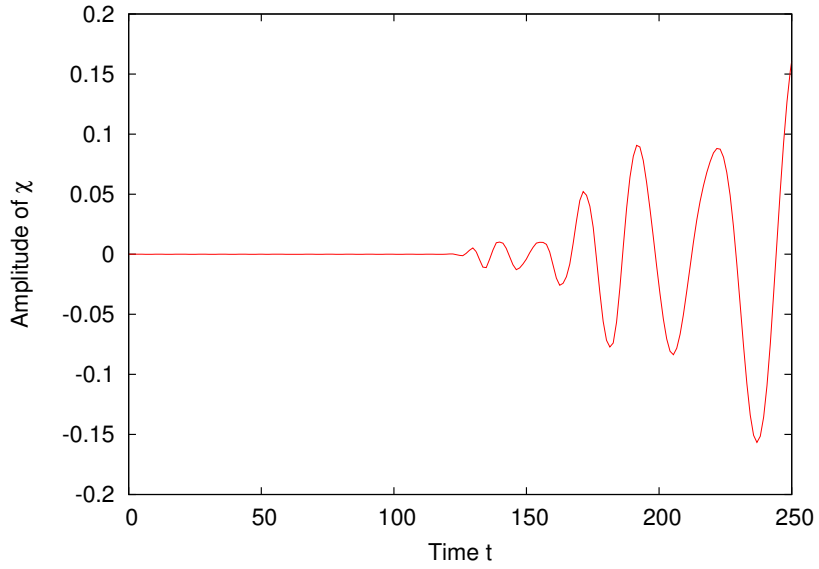


**Figure 3.6.8:** Mean amplitude of $\chi$ in small $\xi$ approximation.

Why does reheating occur in the same way for small values of $\xi$ and $\xi = 0$? Qualitatively, this may be explained by the fact that the inflaton starts close to the Planck scale. Since its evolution $\langle\phi^2\rangle \sim M_{pl}^2/a^2$ and $a$ grows by many order of magnitude, $\langle\phi^2\rangle$ is small at late times. Hence, the non-minimal coupling to gravity will have an irrelevant effect.

Furthermore, these results can be confirmed by analysing the shape of

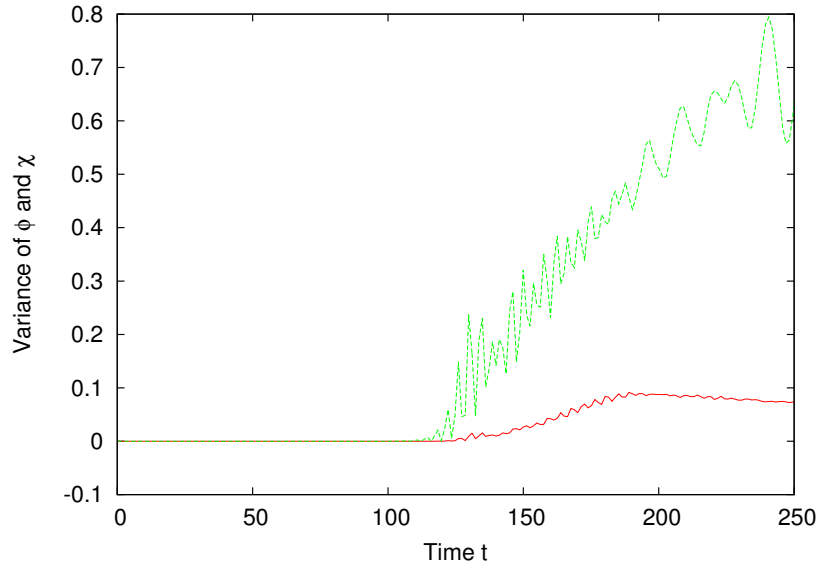


**Figure 3.6.9:** Evolution of the variances $a^2\left(\langle\phi^2\rangle - \langle\phi\rangle^2\right)$ and $a^2\left(\langle\phi^2\rangle - \langle\phi\rangle^2\right)$. The fields are in units of $\phi_0$ and $t$ is the rescaled program time.

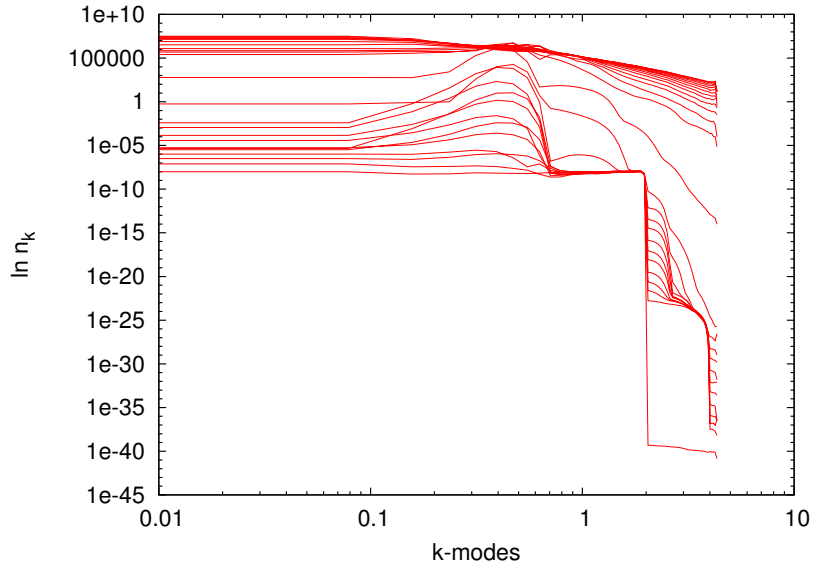


**Figure 3.6.10:** Occupation number $n_\chi$ opposed to momentum modes in logarithmic scale in small $\xi$ aproximation.

the approximate potential in figure 3.6.6 with the potential for $\xi = 0$ in figure 3.6.1. One can notice that for small values of $\phi$ or until the potential in 3.6.6 doesn't drop, the form of the potential is very similar. Since we found analytically that the small $\phi$ approximation and the small $\xi$ approximation

are equivalent, the range of $\xi$ and $\phi$ in our simulations are in fact those in which the potential 3.6.6 and 3.6.1 have the same shape. Thus, it is not a surprise that in that range of the fields, the non-minimal coupling and the minimal coupling regimes have no significant difference.

What is the implication of this result? In previous studies, the minimal coupling quartic model was ruled out of realistic inflationary models. Cosmologists agreed that a non-minimal coupling to gravity is necessary where $\xi$ must obey the constraint $\xi < -0.0019$ imposed by Planck's data. This result shows that all simulations and predictions carried out for the minimal coupling case agree with the data of a model which includes a small non-minimal coupling term and which is compatible with observations. Thus, the results obtained from studying quartic potential in a minimal regime need not to be ruled out, as opposed to its originating theory. In other words, many years of work of an incorrect model do not result to be vain.

# 4. Gravitational Waves

In the previous chapter we have discussed the process of reheating in detail. Gravitational waves are a consequence of its phenomenology. In this chapter I will firstly describe qualitatively gravitational waves, their origin, their significance and the technology we have to detect them directly and indirectly. I will then focus on gravitational wave production during reheating. Finally, I will compute numerical lattice simulations using a further modified MPI/C++ version of LatticeEasy which will simulate the production of gravitational waves during reheating. Again, the aim will be to find how a non-minimally coupling between matter and gravity affects this phenomenon.

## 4.1 The Origin of Gravitational Waves

We expect the Universe to be living in an anisotropic gravitational wave background of either cosmological or astrophysical origin even though it hasn't been detected yet [23]. Astrophysical sources may be collapsing neutron stars and supernovae, merging of galaxies and extreme mass ratio inspirals. As for cosmological sources, we predict a gravitational wave background from inflation, thermal phase transitions at the very early stages of the Universe and for instance, the dynamics of cosmic strings and domain walls [20]. In fact, each phase transition that the Universe undergoes produces a very specific form of gravitational wave background.

One interesting point is that when the gravitational wave backgrounds have been produced by different phenomena, they differ significantly between each other in their spectral shape and frequency [55]. Therefore, if gravitational waves were to be detected, their properties would allow cosmologists to determine its origin precisely. In addition, gravitational waves decouple the moment they are being produced [56]. This means that they don't interact or evolve in time, but they propagate freely and the information they carry will propagate without being disturbed or lost.

Therefore, if we could observe them directly, they would also carry information on the era in which they have been produced. In particular, this is why the detection of primordial gravitational waves would give an enormous contribution to our understanding of the early Universe. It would carry faithful and clear information on the process which generated them and

therefore on the whole dynamics of that specific epoch [57]. Gravitational waves which have been produced during reheating could be the only direct proof of what truly happened during reheating and inflation and therefore our only hope to find a unique theory of the very early Universe.

**"Do Gravitational Waves exist?"**
Einstein published a concrete theory of gravitational waves in 1918 [22] but many physicists were sceptical about the existence of those. For a brief time, Einstein himself changed his opinion; he published in 1937 a paper "*Do Gravitational Waves exist?*", in which he (wrongly) disproved the existence of gravitational waves [22].

Only in the 1970s, after years of discussions, physicists reached consensus that gravitational waves do in fact exist. It was hard to believe in something which is almost directly undetectable. However, many experiments have indirectly proven the existence of gravitational waves, most famous the discovery of the binary pulsar PSR B1913+16, or the "Hulse-Taylor binary pulsar". The Hulse-Taylor binary pulsar was the very first indirect evidence of the existence of gravitational waves [58]. In 1974, Russell Hulse and Joseph Taylor discovered the signal of a pulsar at the Arecibo Observatory in Puerto Rico. They observed periodic changes to the pulsar's pulsation period which implied it was part of a binary system. Observations showed that the orbit of the pulsar is gradually decreasing; in fact the two objects are rotating faster and faster around each other in a smaller and smaller orbit.

According to Einstein's theory of relativity, masses moving relatively to each other should be emitting energy in the form of gravitational waves. The amount of energy loss predicted by Einstein's theory resulted to be in agreement with the decay of the pulsar's orbit. Hence, the emission of gravitational waves from the pulsar binary system was (indirectly) proved to exist as Einstein predicted. Hulse and Taylor won the Nobel Prize in Physics in 1993 for their outstanding discovery.

## 4.2 Gravitational Waves Detectors

It is quite unfortunate how on the one hand we discovered the importance of gravitational waves and on the other we have no currently built observatory able to detect them.

Why is it so hard to detect gravitational waves directly? First of all, as mentioned before, gravity couples very weakly to matter, making it hard for us to detect such low frequencies. Most of the gravitational waves produced result to be very very weak. In order to have strong gravitational waves, one needs massive objects moving very fast (close to the speed of light) [55]. This can happen for instance if the source of the gravitational waves is a black hole.

However, even if gravitational waves are strong, the fractional strain at Earth, i.e. the fractional distortion of an object, caused by a gravitational wave of amplitude h, is of order $h = \Delta L/L \sim 10^{-22}$, over 1km of length. Thus, the fractional change is so small that detectors with very high sensitivity are required.

The first gravitational waves detector was developed in 1960 by Joe Weber. In 1969, he announced to have detected gravitational waves which soon after resulted to be simply noise [59]. Direct observations of gravitational waves have not been made so far. Modern gravitational wave detectors use the technique of laser interferometry in order to try and detect such weak effect. Interferometers are wide-band detectors which can detect frequencies within the range of a few Hz up to a few kHz. The seismic noise dominates at low frequencies and it sets the lower limit of the frequency bands.

The main interferometers that have been built are LIGO (Washington and Louisiana), VIRGO (Pisa, Italy), GEO600 (Hannover) and TAMA300(Japan) [60]. LIGO(Laser Interferometer Gravitational-wave Interferometer) is the largest of gravitational wave detectors and it consists of two interferometers, one in Washington and one in Louisiana [24]. When gravitational waves interact with matter, they stretch and compress objects in one direction and in the perpendicular direction, respectively. The detectors are made of L-shaped 4 kms long arms and they measure the relative lengths of the arms using interferometry. To do this, photons are sent in tubes which travel in the two different arms and reflect several times. If a gravitational wave was to slightly stretch or compress one of the arms of the detector, the interferometer would output a light pattern encoding information on the length change of the arms. Instead, if no gravitational wave is detected, the interferometer will produce no signal since the photon beams in the two arms will cancel each other.

An advanced version of the LIGO experiment, Advanced LIGO, with advanced strain sensitivity and improvement in its isolation, is expected to be replacing LIGO in 2015 [61] and will hopefully be able to detect a broader range of gravitational waves frequencies.

In collaboration with LIGO, another ground based interferometer is VIRGO, built in Cascina, near Pisa [62]. It is also formed by L-shaped 3 kms long arms. Its frequency range extends from 10 to 6000 Hz, which corresponds to gravitational waves produced by supernovae and coalescence of binary systems.

As for space-based gravitational waves, the eLISA( Evolved Laser Interferometer Space Antenna) in 2034 will be the first observatory in space to detect gravitational waves [63]. eLISA should be able to directly observe gravitational waves by measuring the changes of distance between massive objects in a spacecraft. It will be formed by three spacecrafts orbiting the sun forming a high precision interferometer. eLisa will measure how spacetime stretches or compresses giving direct information on gravitational waves.

The advantage of a space-based detector over ground-spaced detectors such as LIGO and VIRGO, is that it will be able to cover the much wider frequency range between 0.1mHz and 1Hz [63]. Moreover, the ground-based detectors have armlength limitations and terrestrial noise. Instead, in space eLISA avoids both seismic and gravity-gradient noise. Its best sensitivity will although be between 3 and 30mHz. Furthermore, LISA will be sensitive to changes in various directions. This will allow it to detect the isotropy of the gravitational wave background and differentiate between a signal of cosmological or astrophysical origin.

## 4.3 Gravitational Waves from Reheating

The source of gravitational waves I am interested in this thesis is that of the decay of coherent oscillations of a field in the phase of reheating. I will be considering the usual quartic model $\lambda\phi^4$ with an interacting potential $g^2\phi^2\chi^2/2$. Then, I will extend such model to non-minimal coupling with gravity and compare it to the previous model.

As discussed in the previous chapter, in the quartic model $\lambda\phi^4$ with an interacting potential $g^2\phi^2\chi^2/2$, coherent oscillations of the scalar field $\phi$ produce fluctuations of the scalar field $\chi$ via parametric resonance. The fluctuations are amplified in a way such that they become classical. The interaction between these fluctuations and the oscillating background, which we call rescattering, produces gravitational radiation [57].

As discussed in chapter 3, parametric resonance occurs only within a certain range of momentum modes $\Delta\kappa$, depending on the choice of parameter $g^2/\lambda$. In position space, this corresponds to field inhomogeneities of size $\Delta L \sim 1/\Delta k$. Due to the inhomogeneous nature of the field, the stress tensor develops an anisotropic nature in which it evolves. It is the transverse-traceless part of the stress tensor which acts as a very efficient source of gravitational waves [54]. More gravitational waves are produced once the inhomogeneous configurations of size $\Delta L$ collide forming smaller inhomogeneities. The production of gravitational waves ends once the field stops oscillating and the GWs decouple from the matter fields and freely propagate towards us.

Mathematically, in order to take into account for inhomogeneities one must consider the full metric of spacetime. The total metric consists of a homogenous and isotropic part and the addition of a small perturbation [27],

$$ds^2 = a^2(t)(\eta_{\mu\nu} + h_{\mu\nu})dx^\mu dx^\nu, \tag{4.3.1}$$

where $\eta_{\mu\nu} = diag(-,+,+,+)$ and $h_{\mu\nu}$ is the perturbation. We are only interested on the transverse and traceless part of the perturbations since they act as a source of gravitational waves. Hence, we must impose the constraints $\partial_i h_{ij} = h_{ii} = 0$ on the metric perturbation which guarantees transversality and tracelessness (we can therefore neglect the TT superscript of $h_{ij}$).

Considering the whole metric above and linearizing the Einstein equations, the transverse-traceless(TT) part yields the equation of motion for the perturbations [54] ,

$$\ddot{h}_{ij} + 3H\dot{h}_{ij} - \frac{1}{a^2}\nabla^2 h_{ij} = \frac{16\pi}{M_{pl}^2 a^2}\Pi_{ij}^{\mathrm{TT}}(\phi, \chi). \tag{4.3.2}$$

Assuming no gravitational production at the start of reheating $t = t_i$, the solution to the GW equation above is given by a causal convolution with appropriate Green's function [57],

$$h_{ij}(t, \mathbf{k}) = \frac{16\pi}{M_p^2}\int_{t_i}^{t} \mathcal{G}(t, t')\Pi_{ij}^{\mathrm{TT}}(t', \mathbf{k}). \tag{4.3.3}$$

Therefore, all there is to find is the corresponding Green's function $\mathcal{G}(t, t')$ and $\Pi_{ij}^{TT}$, the traceless-transverse part of the spatial components of the anisotropic stress tensor, the source of gravitational waves. Hence, the conditions $\partial_i \Pi_{ij}^{\mathrm{TT}} = \Pi_{ii}^{\mathrm{TT}} = 0$ must also hold.

It is hard to give an explicit derivation of the anisotropic stress tensor $\Pi_{ij}^{\mathrm{TT}}$. Thus, we can think of the full stress energy tensor as the sum of the anisotropic part $\Pi_{ij}$ and the isotropic part, which is given by the pressure of the homogenous background [64]. Hence we can define $\Pi_{ij}$ as,

$$a^2\Pi_{ij} = T_{ij} - \langle P \rangle g_{ij}, \tag{4.3.4}$$

where P is the homogenous background pressure and the stress energy tensor is given by the usual form,

$$T_{\mu\nu} = \partial_\mu\phi\partial_\nu\phi - g_{\mu\nu}\mathcal{L}. \tag{4.3.5}$$

Hence, by substituting in equation (4.3.4) expressions for $T_{ij}$ for both $\phi$ and $\chi$, one obtains the expression for the full anisotropic stress tensor,

$$\Pi_{ij} = \frac{1}{a^2}[\partial_i\phi\partial_j\phi + \partial_i\chi\partial_j\chi - g_{ij}(\mathcal{L} + \langle P \rangle)]. \tag{4.3.6}$$

To find the TT projection of $\Pi_{ij}$ and to study the fluctuations, I will use the formalism introduced in [64]. This method works in Fourier space, so firstly I will transform equation (4.3.2) in momentum space. I will use the Fourier space convention,

$$\tilde{f}(t, \mathbf{k}) = \int d^3\mathbf{x} f(t, \mathbf{x}) e^{-i\mathbf{k}\mathbf{x}}. \tag{4.3.7}$$

The equation of motion for the fluctuations in momentum space becomes,

$$\ddot{h}_{ij}(t, \mathbf{k}) + 3H\dot{h}_{ij}(t, \mathbf{k}) - \frac{k^2}{a^2}h_{ij}(t, \mathbf{k}) = \frac{16\pi}{M_{pl}}\Pi_{ij}^{\mathrm{TT}}(t, \mathbf{k}). \tag{4.3.8}$$

In momentum space, the TT projection of the anisotropic stress tensor can be obtained using a projector operator such that [65],

$$\begin{aligned}\Pi_{ij}^{\mathrm{TT}}(t,\mathbf{k}) =& \Lambda_{ij,kl}(\hat{k})\Pi_{ij}(t,\mathbf{k}) \\ =& \Lambda_{ij,kl}(\hat{k})\int d\mathbf{x}e^{-i\mathbf{kx}}[\partial_l\phi\partial_m\phi+\partial_l\chi\partial_m\chi](t,\mathbf{x}),\end{aligned} \tag{4.3.9}$$

where,

$$\begin{aligned}&\Lambda_{ij,kl}(\hat{k}) = P_{il}P_{jm}-\frac{1}{2}P_{ij}P_{lm}, \\ &P_{ij}\equiv\delta_{ij}-k_ik_j/k^2.\end{aligned} \tag{4.3.10}$$

The operator $\Lambda_{ij,kl}(\hat{k})$ projects onto the subspace orthogonal to $\mathbf{k}$, such that $P_{ij}k_i = P_{ij}P_{jl} = 0$, which indeed implies that it projects the TT part of $\Pi_{ij}$. In other words, the conditions on $P_{ij}$ imply the conditions of transversality and tracelessness on $\Pi_{ij}$, $\Pi_{ij}^{\mathrm{TT}}k_j = \Pi_{ii}^{\mathrm{TT}} = 0$. Notice that when taking the TT projection, the term proportional to the metric in (4.3.6) disappeared. This is because that term turns out to be of second order in $h_{ij}$, which we can neglect. Therefore, we find explicitly that the gradients of the fields are the source of gravitational waves.

It is possible to use a method in which we can solve equation (4.3.2) without having to compute the Green's function. In fact, from a numerical point of view, it would be highly inconvenient for the program to find the TT projection of $\Pi_{ij}$, Fourier transform to momentum space and back to configuration space, at each time step. This involves non-local operations which are computationally very costly. Therefore, in section 4.4 I will present a method which simplifies the numerical simulations, introduced for the first time in [57].

The energy density $\rho_{\mathrm{GW}}$ is a physical quantity which carries information on the amount of energy carried by the gravitational waves. The energy-momentum tensor of the GW is given by [56],

$$t_{\mu\nu} = \frac{M_p^2}{32\pi}\langle\partial_\mu h_{ij}\partial_\nu h^{ij}\rangle_V, \tag{4.3.11}$$

where the TT tensor perturbations $h_{ij}$ satisfy equation (4.3.2) and the expectation value $\langle..\rangle_V$ is taken over a volume $V = L^3$ such that the measure of GW energy-momentum tensor is gauge invariant. The gravitational density is defined as the 00-component of the stress energy tensor, i.e. $\rho_{\mathrm{GW}} = t_{00}$. Thus, the energy density averaged over a volume $V = L^3$ is,

$$\rho_{\mathrm{GW}} = \frac{M_p^2}{32\pi L^3}\int d^3x\dot{h}_{ij}(t,\mathbf{x})\dot{h}_{ij}^*(t,\mathbf{x}) = \frac{M_p^2}{32\pi L^3}\int\frac{d^3k}{(2\pi)^3}\dot{h_{ij}}(t,\mathbf{k})\dot{h}_{ij}^*(t,\mathbf{k}). \tag{4.3.12}$$

The spectrum of gravitational waves per logarithmic frequency is then given by [54],

$$\frac{d\rho_{\rm GW}}{d\log k} \equiv \frac{k^3 M_p^2}{(4\pi L)^3} \int \frac{d\Omega_k}{4\pi} \dot{h}_{ij}(t,\mathbf{k}) \dot{h}^*_{ij}(t,\mathbf{k}). \tag{4.3.13}$$

Thus, one can obtain the total energy density of gravitational waves normalized by the critical density,

$$\Omega_{\rm GW}(t) = \frac{1}{\rho_{GW}} \int \left( \frac{d\rho_{GW}}{d\log k} \right) d\log k. \tag{4.3.14}$$

## 4.4 Numerical Simulations

One of the main purposes of this thesis is to study the effects on gravitational waves production of a reheating background where the scalar fields are non-minimally coupled to gravity. I will be computing 3D lattice simulations in order to give a numerical estimate on the gravitational wave spectrum generated during reheating by the same chaotic model I have been discussing throughout this thesis.

I made use of a further modified version of LatticeEasy which included a code to reproduce the gravitational wave spectra at different time steps. It is an MPI/C++ code which was firstly formulated by Daniel G. Figueroa [66] and which was passed on to me by Laura B. Bethke [67]. An MPI code is parallelised such that several CPUs run the code at the same time which makes the simulation faster. The main change in this version of the code is that it includes a function which calculates the normalised gravitational wave spectrum of equation (4.3.13). This function is determined by the evolution of the transverse traceless tensor perturbation given by equation (4.3.2) . Hence, the code now involves the fields $\phi$ and $\chi$ and the six tensor perturbations components $h_{ij}$ producing the gravitational waves and acting as 'fields'.

As discussed when computing simulations on the dynamics of reheating, the numerical algorithm used by the LatticeEasy package to solve the differential equations is a leapfrog integrator which stores the field values and its derivatives at each time step.

In principle, the code would perform the TT projection of equation (4.3.8), solve the equations in Fourier space and then transform back to coordinate space. As one would expect, this is computationally very costly. The code I will be using is instead based on a method which avoids this and which was introduced in [57]. I will present their method in the following discussion.

We have seen that the solution to equation (4.3.2) can be written in terms of a Green function as in equation (4.3.3). However, recall that one can write the TT projection of the anisotropic stress tensor in terms of the projector defined in (4.3.10), as in equation (4.3.9). Now, notice that the solution in (4.3.3) is linear in $\Pi_{ij}^{\rm TT}$ and can therefore be written as [66],

$$h_{ij}(\mathrm{k},t) = \Lambda_{ij,kl}(\hat{\mathbf{k}})\frac{6\pi}{M_{pl}^2}\int_{t_i}^{t}\mathcal{G}(t,t')\Pi_{lm}(t',\mathbf{k}). \tag{4.4.1}$$

This allows us to redefine $h_{ij}$ in terms of a function $u_{ij}(\mathbf{k},t)$, such that [66],

$$h_{ij}(\mathbf{k},t) = \Lambda_{ij,kl}(\hat{k})u_{ij}(\mathbf{k},t), \tag{4.4.2}$$

where $u_{ij}(\mathbf{k},t)$ is given by,

$$u_{ij}(\mathbf{k},t) = \frac{6\pi}{M_{pl}^2}\int_{t_i}^{t}\mathcal{G}(t,t')\Pi_{lm}^{\mathrm{eff}}(t',\mathbf{k}). \tag{4.4.3}$$

Here, I have introduced the effective anisotropic stress tensor $\Pi_{ij}^{\mathrm{eff}}(\mathbf{k},t')$, given by the Fourier transform of the unprojected source term [67],

$$\Pi_{ij}^{\mathrm{eff}}(\mathbf{x},t') \equiv \frac{1}{a^2}\left[\partial_i\chi\partial_j\chi + \partial_i\phi\partial_j\phi\right](\mathbf{x},t). \tag{4.4.4}$$

Hence, the function $u(\mathbf{k},t)$ is simply the solution of the equation,

$$\ddot{u}_{ij} + 3H\dot{u}_{ij} - \frac{1}{a^2}\nabla^2 u_{ij} = \frac{16\pi}{M_{pl}^2}\Pi_{ij}^{\mathrm{eff}}(\phi,\chi). \tag{4.4.5}$$

Notice that the solution $u(\mathbf{k},t)$ doesn't involve the TT projection. Thus, one can avoid to perform the TT projection explicitly at each time step by letting the simulation solve the equation of motion for $u(\mathbf{k},t)$ in (4.4.5).

In this way, we will only Fourier transform $u_{ij}(\mathbf{x},t)$ to $u_{ij}(\mathbf{k},t)$ and find the corresponding $h_{ij}(\mathbf{k},t)$ via equation (4.4.2) when we want to compute real physical TT degrees of freedom $h_{ij}$. Thus, in any moment of the evolution, we can obtain the gravitational wave spectrum which is determined by $\dot{h}_{ij}$ via equation (4.3.13).

As mentioned before, LatticeEasy solves discretized versions of the equations. Therefore we will have to find a discretized version of equation (4.3.12) which the program can solve. Using $L^3 = (N\delta x)^3$, where N is the number of lattice points and $\delta x = L/N$ is the lattice spacing, and a discrete position vector $\mathbf{n} = (n_1, n_2, n_3)$, one can write equation (4.3.12) as [67],

$$\rho_{GW} = \frac{M_p^2}{32\pi N^3}\sum_{n}\dot{h}_{ij}(t,\mathbf{n})\dot{h}_{ij}^{*}(t,\mathbf{n}). \tag{4.4.6}$$

Using the discrete Fourier transform convention $f(\mathbf{n}) = 1/N^3\sum_n e^{-\frac{2\pi i}{N}\tilde{\mathbf{n}}\cdot\mathbf{n}}\tilde{f}(\tilde{\mathbf{n}})$ and the discrete form of the delta function $\sum_n e^{-\frac{2\pi i}{N}(\tilde{\mathbf{n}}-\tilde{\mathbf{n}}')\cdot\mathbf{n}} = N^3\delta(\tilde{\mathbf{n}}-\tilde{\mathbf{n}}')$, one obtains an equivalent expression in Fourier space,

$$\rho_{GW} = \frac{M_p^2}{32\pi N^6} \sum_{\tilde{n}} \dot{h}_{ij}(t, \tilde{\mathbf{n}}) \dot{h}^*_{ij}(t, \tilde{\mathbf{n}}). \tag{4.4.7}$$

### Numerical parameters

As for the simulations on the dynamics of reheating, in order to carry out simulations on the gravitational wave production, one has to firstly choose the appropriate numerical parameters.

The lattice size L must be determined by the infrared momentum $k_{\mathrm{IR}} = \frac{2\pi}{L}$, corresponding to the largest wavelength that fits in the lattice box. A large enough lattice spacing will ensure good IR coverage. However, a good UV coverage is also needed. This improves with the number of lattice points N, which sets the lattice spacing $\delta x = L/N$. This has to be smaller than any relevant length scale in order for all the relevant physics to fit within the lattice size. I will show how different choices of $N$ and $L$ influence the reliability of the simulations. After multiple trials, I found that the choice of $N = 128$ and $L = 50$ is the appropriate choice ot obtain valid simulations on gravitational wave production in my model.

As in the previous chapter, I chose the value of the inflaton's self coupling to be $\lambda = 9 \times 10^{-14}$, consistent with WMAP data [7] and $g^2/\lambda = 1$. The initial condition of the scale factor is chosen to be $a_i = 1$ and the amplitude of the inflaton as $\phi_0 = 0.342 M_{pl}$, just as in the previous simulations. Recall that just as before, the program fields are given in units of $\phi_0$ and rescaled by a factor of $a$.

To find the initial value of the field $\chi$ one must explore in more details its properties. The lightness of $\chi$ implies that at the end of inflation and during preheating it will vary on superhorizon scales. This means that each Hubble volume will have its own non-zero background value of $\chi_i$. This consideration makes use of the so called *separate universe approximation* for non-linear superhorizon perturbations [68]. Every quantity that depends on $\chi_i$ will vary between the different Hubble volumes. It was found that the production of gravitational waves depends sensitively on the initial value $\chi_i$ and numerical simulations were done to study the dependence of $\Omega_{\mathrm{GW}}$ on $\chi_i$[54]. Within certain ranges of values of $\chi_i$, $\Omega_{\mathrm{GW}}$ has a chaotic behaviour. In this scenario, the production of GWs is highly sensitive to the particular value of $\chi_i$. Even though this results to be a more interesting scenario since it is a very efficient regime of gravitational wave production, it is not in the interest of this thesis to discuss the effect of $\chi_i$ on $\Omega_{\mathrm{GW}}$. Therefore, I chose $\chi_i = 0$, where $\Omega_{\mathrm{GW}}$ is least sensitive to $\chi_i$. Unfortunately, under this condition, the gravitational waves produced have the smallest amplitude.

### 4.4.1 Simulations on Gravitational Wave Production

**Minimal-coupling case**

Figure 4.4.1 shows the evolution of $\Omega_{\rm GW}$ during reheating. The gravitational wave production starts as the field $\chi$ grows exponentially due to parametric resonance with the field $\phi$. The gravitational wave amplitude grows of many orders of magnitude.

Figure 4.4.1 reproduces the GW spectra at different times for the choice of lattice size $L$ and number of lattice points $N$, such that L=60 and N=64. One can notice that in the UV range (large wave number $k$) the amplitude at late time is not highly suppressed since it only falls off to about $10^{-5}$. This means that the plot cannot be fully trusted since we cannot assure that all relevant physics is captured.

In order for the plot to not be dependent on the choice of lattice parameters, one must make sure that the choice of N,L allows all relevant physics to be reproduced.

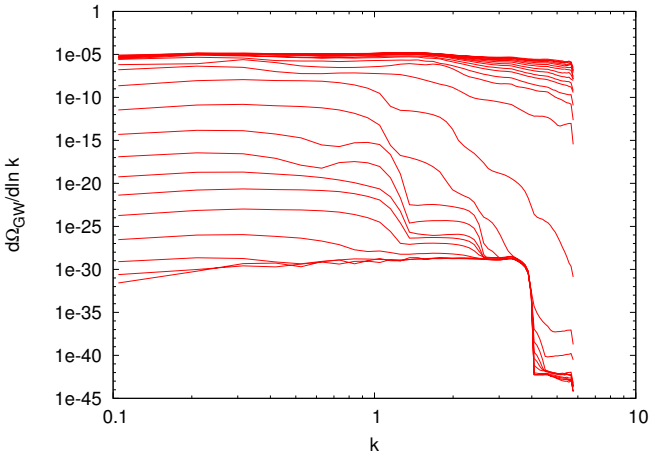


**Figure 4.4.1:** Gravitational wave spectra with N=64,L=60

I therefore chose to decrease $L$ and increase $N$ such that $N = 128$ and $L = 50$ (figure 4.4.2) in order to increase the lattice spacing. In this case, one can notice that in the UV range the spectrum falls off and it is therefore not dominated by lattice effects.

Gravitational wave production becomes significant once the system becomes non-linear. This is because gravitational waves are sourced by the field's gradients and in this regime the gradients become larger corresponding to higher GWs intensity. At the end of parametric resonance, when the fields both have small amplitudes (and even if they're still slightly oscillating), the GW production ceases and the amplitude saturates. That final amplitude is what we should find today if this kind of gravitational wave background was to be observed. After parametric resonance, the fields enter a turbulent

stage in which GWs are not being produced [57].

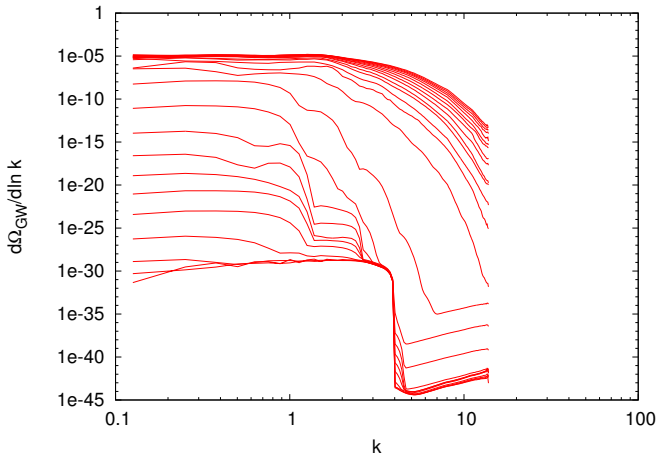


**Figure 4.4.2:** Gravitational wave spectra with N=128,L=50

### Non-minimal coupling case: small $\xi$ approximation

Figure 4.4.3 shows the GW spectra at different time steps during reheating for the non-minimally coupled model. I chose again values of the lattice parameters $L = 50$ and $N = 128$ in order to assure that the UV range would be highly suppressed. One can easily notice the strong similarities to the minimal coupling case. The amplitude is increased by several orders of magnitude during parametric resonance until it reaches saturation at the end of parametric resonance.

This confirms the results obtained by simulating the evolution of the non-minimally coupled fields during reheating. We saw that in the small $\xi$ approximation, the addition of the non-minimally coupled term had no effect on their dynamics. Therefore, parametric resonance occurred in the same way and the exponential growth of $\chi$ also occurred reasonably similarly. From figure 4.4.3 we see that the gravitational wave production is also not being affected by the non-minimal coupling between matter and gravity, at least for the small $\xi$ approximation. This was to be expected since if the reheating process follows the same dynamics, then also the gravitational wave production will occur in the same way.

What does this similarity imply? We found that the minimal regime and the non-minimal one for small values of the coupling predict the same gravitational radiation produced during reheating. Hence, we can conclude that even if $\lambda\phi^4$ theory has been ruled out by Planck's constraints, it agrees with a non-minimal coupling theory which is compatible with Planck's data. This is of strong physical significance because it implies that all predictions from $\phi^4$ theory, that were considered wrong, are actually consistent with the

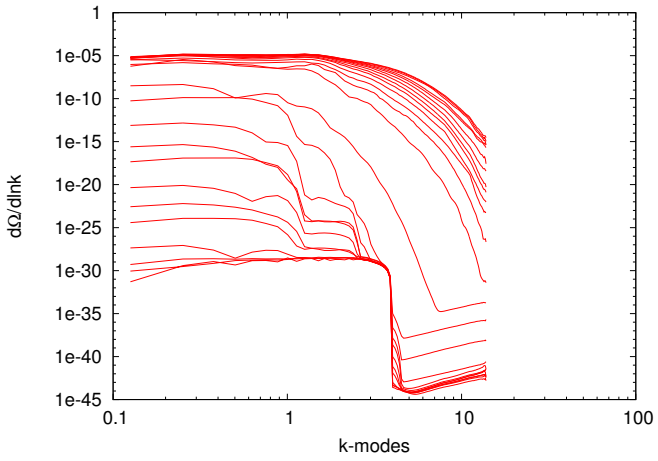


**Figure 4.4.3:** Gravitational wave spectrum in small $\xi$ approximation with N=128,L=50

predictions of a realistic and highly plausible model. This means that the data from $\phi^4$ theory is still to be considered valid.

# 5. Future Improvements

My work is based on several approximations in order to simplify calculations yet still presenting valid results. An improvement could be made if for instance one was able to find the exact rescaling of the fields $\phi$ and $\chi$ when conformally transforming the action from the Jordan to the Einstein frame in section (3.5.2). In my case, this couldn not be found since I assumed flat FRLW metric although realistically spacetime is curved. My assumption of flat FRLW spacetime implied that the action in the Einstein frame did not include a cross term of the form $K\partial_\mu\tilde{\phi}\partial^\mu\tilde{\chi}$ where $K$ is some curvature-dependent function.

Instead, if a curved spacetime was to be considered, a non-zero cross term would have to be considered in the action and one could obtain an exact rescaling of the fields $\phi$ and $\chi$. However, this would make calculations even more complicated. Therefore, I tried to obtain a more accurate result by including the cross term in the Einstein frame action even though assuming flat spacetime but exact rescalings also failed to exist. In conclusion, the only way to predict exact solutions would be to go the complicated way and consider the curvature in the metric.

Note also that the equations of motion which LatticeEasy is built to solve are those in equation (3.6.1), which are derived from an action which does not include the cross term. Thus, if one was to include the cross term in the action then it would be necessary to modify LatticeEasy in order for it to solve the equations of motions yielded by such an action.

My work can be further improved even within the approximation I have made. In my disussion of reheating in the small $\xi$ approximation, I have considered only first orders in $\xi$. It would be interesting to study the dynamics of reheating up to higher orders in $\xi$ and to see if this agrees with the first order approximation I have made in my discussion. As found for the first order approximation, we expect the effect of the non-minimal coupling in this approximation to also be negligible for higher orders of $\xi$. However, the results would be more accurate and hence more reliable.

Due to the limited amount of time I had to carry out this work, I did not have time to numerically study reheating in the large $\phi$ approximation. This can be done in a similar way to that in the small $\xi$ approximation. The major changes involve of course the potential and its derivatives with respect

to $\phi$ and $\chi$ which set the evolution of the fields and of the scale factor and which we found analytically to be given by equations (3.5.42) ,(3.5.43) and (3.5.44), respectively. Just as in the small $\xi$ approximation, one must rescale the variables into program variables in a computationally convenient form.

In this regime the inflaton inflates for longer and its value when it ends inflation and enters reheating will be smaller compared to that in the small $\xi$ approximation. This can be explictly seen in figure 3.5.1 where we notice the longer flat slope of the potential and that the inflaton rolls down towards the minimum much later than in the small $\xi$ approximation (figure 3.6.6).

Since inflation ends when either one of the two slow-roll parameters $\epsilon$ and $\eta$ are of order 1, the value of the inflaton as it enters reheating is simply that for which such condition is satisfied. In other words, we are looking for the value of $\phi$ which satisfies,

$$\epsilon \equiv \frac{1}{16\pi G}\left(\frac{V'}{V}\right)^2 \simeq 1. \tag{5.0.1}$$

Since we take the initial value $\chi_0 = 0$, the potential in equation (3.5.42) can be simplified to the form,

$$V = \frac{\lambda}{4\kappa^4\xi^2}\left(1 - e^{-\sqrt{\frac{2}{3}}\kappa\tilde{\phi}}\right)^2, \tag{5.0.2}$$

where $\kappa^2 = 8\pi G$. Using this potential $V$ to recover $\epsilon$, one finds that $\epsilon \simeq 1$ when $\tilde{\phi} \simeq \sqrt{\frac{3}{2}}\frac{1}{\kappa}\ln\left(1 + \frac{2}{\sqrt{3}}\right)$. Setting this value (in program variables) as the initial condition for the inflaton will assure that the program is simulating the evolution fo the fields during their stage of reheating.

In my opinion, since the non-minimal coupling in this approximation results to be strong, one should expect to find changes on the phenomenology of reheating compared to the minimal coupling case. Consequently, the production of graviational waves would also be affected since it strongly depends on the dynamics of reheating.

Moreover, approximations in the small $\xi$ regime and in the large $\phi$ regime would allow us to make an educated guess on the form of the full potential. Thus, using an ansatz, one could study the dynamics of reheating for any value of the fields and the coupling $\xi$ (always complying with the restrictions given by the latest experimental results, which today are Planck's 2013 results).

Last, but not least, my model could be generalised if one considers two different coupling between gravity and the two fields. This would allow us to choose independentely the strength of interaction between gravity and each of the two fields.

# 6. Conclusions

Throughout this thesis, I presented analytical and numerical discussions on the theory of reheating and on its phenomenological consequence of gravitational wave production. I chose to study these aspects of the early Universe in a particular inflationary theory which had not been discussed before. I chose a quartic chaotic model involving two interacting massless scalar fields, both non-minimally coupled to gravity. Pure $\lambda\phi^4$-theory had been ruled out by Planck's observations. I chose to generalise this theory to a realistic model, compatible with observations, which accounts for interactions between matter and gravity. This model turned out to have some very interesting physical implications.

The aim of this discussion was to study the effect of the matter-gravity interaction on reheating and on the production of gravitational waves during that time. In order to study this effect I chose to compare such a model with a minimally coupled one. I performed lattice simulations on the behaviour of the fields during reheating which clearly showed the effects of the parametric resonance. The oscillating nature of the inflaton induces the field $\chi$ to grow exponentially. This corresponds to an increase in the number occupation of $\chi$-particles. Due to the significant amount of energy transfer from $\phi$ to $\chi$, $\chi$ will eventually reach an amplitude similar to $\phi$ and they will enter a non-linear regime which sets the end of the parametric resonance.

Gravitational wave production starts due to field inhomogeneities arising from $\chi$'s growth and becomes significant once the system becomes non-linear. Graviational waves intensity becomes larger in the non-linear regime due to the field's gradients being much larger and power being transferred to higher momenta. Once gravitational wave production reaches an end, the amplitude of gravitational wave saturates and that results to be the final gravitational wave background we expect the Universe to be filled with today.

I focused on numerical 3D lattice simulations for small values of the non-minimal coupling $\xi$. These simulations showed a strong correlation with those of the minimally coupled case. The reheating process follows the same dynamics and therefore would produce the same gravitational wave background. As a consequence, even if $\lambda\phi^4$-theory has been ruled out, we have that its predictions can still be considered valid. This result is of strong significance since it implies that all the data recovered from $\phi^4$- theory should

still be taken into account. How can two theories, one incompatible and one compatible with observations, predict the same results? There is clearly still much to discover from this model.

The answer will probably arise only with further improvements in our tehnology. Currently, we are not able to detect this kind of gravitational wave background directly. If measurements became possible, one could provide further constraints to inflationary models and explain how the preheating regime occurs. It is possibly the only direct information from the very early Universe which is present in our Universe since it has been decoupled since the moment of its production and therefore the information it carries has not been disrupted by the evolution of the Universe. Its spectra provides a direct picture of the reheating process of the Universe. It would therefore provide an enormous contribution to the development of a theory of the very early Universe.

However, our current gravitational wave detectors are not sensitive enough to cover the frequency ranges of primordial gravitational waves. The BICEP2, which studies the B-mode polarizations of the CMB, is the first attempt to study primordial gravitational wave backgrounds and future developments of it could improve our understanding of these perturbations [26]. We hope that future planned observatories will be able to detect primordial gravitational wave backgrounds. In particular, if inflation occured at low-scales, observatories such as BBO may be able to detect the gravitational wave background arising from preheating [69].

Finally, a quantum theory of gravity [70] together with observational improvements will hopefully lead us to find a unique theory on the creation and the events which followed in the first fractions of a second.

# Bibliography


[1] J. A. Peacock, *Cosmological Physics*. Cambridge University Press, 1999.

[2] V. Mukhanov, *Physical Foundations of Cosmology*. Cambridge University Press, 2005. Cambridge Books Online.

[3] A. Liddle, *An introduction to modern cosmology*. Wiley, 2003.

[4] S. Weinberg, *Gravitation and Cosmology*. John Wiley & Sons, 1972.

[5] R. W. Wilson and A. A. Penzias, "Isotropy of Cosmic Background Radiation at 4080 Megahertz," *Science*, vol. 156, pp. 1100–1101, May 1967.

[6] D. Fixsen, E. Cheng, D. Cottingham, R. Eplee, R. Isaacman, *et al.*, "Cosmic microwave background dipole spectrum measured by the COBE FIRAS," *Astrophys.J.*, vol. 420, p. 445, 1994.

[7] D. Spergel *et al.*, "First year Wilkinson Microwave Anisotropy Probe (WMAP) observations: Determination of cosmological parameters," *Astrophys.J.Suppl.*, vol. 148, pp. 175–194, 2003.

[8] P. Ade *et al.*, "Planck 2013 results. XVI. Cosmological parameters," *Astron.Astrophys.*, 2014.

[9] A. D. Linde, "Inflationary Cosmology," *Lect.Notes Phys.*, vol. 738, pp. 1–54, 2008.

[10] "The Best Inflationary Models After Planck," *JCAP*, vol. 1403, p. 039, 2014.

[11] E. Kolb and M. Turner, *The Early Universe*. Frontiers in physics, Westview Press, 1994.

[12] A. D. Linde, "Chaotic Inflation," *Phys.Lett.*, vol. B129, pp. 177–181, 1983.

[13] L. Kofman, A. D. Linde, and A. A. Starobinsky, "Towards the theory of reheating after inflation," *Phys.Rev.*, vol. D56, pp. 3258–3295, 1997.

[14] P. B. Greene, L. Kofman, A. D. Linde, and A. A. Starobinsky, "Structure of resonance in preheating after inflation," *Phys.Rev.*, vol. D56, pp. 6175–6192, 1997.

[15] R. Allahverdi, "Thermalization after inflation and reheating temperature," *Phys.Rev.*, vol. D62, p. 063509, 2000.

[16] M. P. Hertzberg, "On Inflation with Non-minimal Coupling," *JHEP*, vol. 1011, p. 023, 2010.

[17] R. Wald, *General Relativity*. University of Chicago Press, 2010.

[18] A. A. Logunov, M. A. Mestvirishvili, and V. A. Petrov, "FROM THE HISTORY OF PHYSICS: How were the Hilbert-Einstein equations discovered?," *Physics Uspekhi*, vol. 47, pp. 607–621, June 2004.

[19] S. Carroll, *Spacetime and Geometry: An Introduction to General Relativity*. Addison Wesley, 2004.

[20] A. Buonanno, "Gravitational waves." 0709.4682, 2007.

[21] R. W and A. Einstein, *Relativity: The Special and General Theory*. Henry Holt, 1920.

[22] A. Einstein, "Uber Gravitationswellen," *Sitzungsberichte der Koniglich Preussischen Akademie der Wis- senschaften Berlin.*, vol. 154-167, 1918.

[23] E. E. Flanagan and S. A. Hughes, "The Basics of gravitational wave theory," *New J.Phys.*, vol. 7, p. 204, 2005.

[24] B. Abbott *et al.*, "LIGO: The Laser interferometer gravitational-wave observatory," *Rept.Prog.Phys.*, vol. 72, p. 076901, 2009.

[25] P. Collaboration and P. A. R. A. et al., "Planck 2013 results. xxii. constraints on inflation," 2013.

[26] P. Ade *et al.*, "Detection of B-Mode Polarization at Degree Angular Scales by BICEP2," *Phys.Rev.Lett.*, vol. 112, p. 241101, 2014.

[27] S. Khlebnikov and I. Tkachev, "Relic gravitational waves produced after preheating," *Phys.Rev.*, vol. D56, pp. 653–660, 1997.

[28] L. Bergstrom and A. Goobar, *Cosmology and Particle Astrophysics*. Springer Praxis Books / Astronomy and Planetary Sciences, Springer, 2006.

[29] A. Liddle and D. Lyth, *Cosmological Inflation and Large-Scale Structure*. Cambridge University Press, 2000.

[30] D. Langlois, "Inflation and cosmological perturbations." Lectures on Cosmology Accelerated Expansion of the Universe by Georg Wolschin, Lecture Notes in Physics vol. 800, Springer Berlin / Heidelberg, ISSN 1616-6361; ISBN 978-3-642-10597-5, pp.1-57, 2010.

[31] A. Guth, *The Inflationary Universe.* Basic Books, 0 ed., 3 1998.

[32] A. H. Guth, "Inflationary universe: A possible solution to the horizon and flatness problems," *Phys. Rev. D*, vol. 23, pp. 347–356, Jan 1981.

[33] M. Postma, *Inflation.* NIKHEf, Science Park 105 1098 XG Amsterdam, The Netherlands., 2010.

[34] J. Lesgourgues, "Inflationary cosmology," 2006. Lecture notes of a course presented in the framework of the 3ieme cycle de physique de Suisse romande.

[35] D. Baumann, "TASI Lectures on Inflation." 0907.5424, 2009.

[36] C. Contaldi, "Cosmology." University Lectures, Imperial College London, 2012.

[37] P. Peter, "Cosmological Perturbation Theory." arXiv:1303.2509, 2013.

[38] G. N. Felder and I. Tkachev, "LATTICEEASY: A Program for lattice simulations of scalar fields in an expanding universe," *Comput.Phys.Commun.*, vol. 178, pp. 929–932, 2008.

[39] K. R. Meyer, "Jacobi elliptic functions from a dynamical systems point of view," *The American Mathematical Monthly*, vol. 108, no. 8, pp. 729–737, 2001.

[40] B. M. Project, H. Bateman, A. Erdélyi, and U. S. O. of Naval Research, *Higher Transcendental Functions.* No. v. 3 in Higher Transcendental Functions, McGraw-Hill, 1955.

[41] G. Floquet, "Sur les équations différentielles linéaires á coefficients périodiques," *Annales scientifiques de l'École Normale Supérieure*, vol. 12, pp. 47–88, 1883.

[42] J. Strang, "On the characteristic exponents of Floquet solutions to the Mathieu equation," *ArXiv Mathematical Physics e-prints*, Oct. 2005.

[43] L. Pontryagin, *Ordinary differential equations.* Addison-Wesley, 1962.

[44] D. Semikoz, "The kinetic stage of the universe reheating," *Helv.Phys.Acta*, vol. 69, pp. 207–210, 1996.

[45] T. Futamase and K.-i. Maeda, "Chaotic Inflationary Scenario in Models Having Nonminimal Coupling With Curvature," *Phys.Rev.*, vol. D39, pp. 399–404, 1989.

[46] N. Mahajan, "On non-minimal coupling of the inflaton." arXiv:1302.3374, 2013.

[47] C. F. Steinwachs and A. Y. Kamenshchik, "Non-minimal Higgs Inflation and Frame Dependence in Cosmology," *AIP Conf.Proc.*, vol. 1514, pp. 161–164, 2012.

[48] V. Faraoni, E. Gunzig, and P. Nardone, "Conformal transformations in classical gravitational theories and in cosmology," *Fund.Cosmic Phys.*, vol. 20, p. 121, 1999.

[49] R. Fakir and W. G. Unruh, "Improvement on cosmological chaotic inflation through nonminimal coupling," *Phys. Rev. D*, vol. 41, pp. 1783–1791, Mar 1990.

[50] V. Faraoni, "Does the nonminimal coupling of the scalar field improve or destroy inflation?." 7th Canadian Conference on General Relativity and Relativistic Astrophysics(CCGRRA 7). Calgary,Alberta,Canada, 1997.

[51] V. Faraoni, "Conformally coupled inflation," *Galaxies*, 2013.

[52] J. Kim, Y. Kim, and S. C. Park, "Two-field inflation with non-minimal coupling," *Class.Quant.Grav.*, vol. 31, p. 135004, 2014.

[53] F. L. Bezrukov and M. Shaposhnikov, "The Standard Model Higgs boson as the inflaton," *Phys.Lett.*, vol. B659, pp. 703–706, 2008.

[54] L. Bethke, D. G. Figueroa, and A. Rajantie, "On the Anisotropy of the Gravitational Wave Background from Massless Preheating," *JCAP*, vol. 1406, p. 047, 2014.

[55] D. Holz, "Gravitational wave cosmology," January 13-17 2014. Lectures given at Essential Cosmology for the Next Generation/Cosmology on the Beach conference, Cabo San Lucas, Mexico.

[56] M. Maggiore, *Gravitational Waves: Volume 1: Theory and Experiments*. Gravitational Waves, OUP Oxford, 2007.

[57] J. Garcia-Bellido, D. G. Figueroa, and A. Sastre, "A Gravitational Wave Background from Reheating after Hybrid Inflation," *Phys.Rev.*, vol. D77, p. 043517, 2008.

[58] R. Hulse and J. Taylor, "Discovery of a pulsar in a binary system," *Astrophys.J.*, vol. 195, pp. L51–L53, 1975.

[59] J. Weber, "Evidence for discovery of gravitational radiation," *Phys. Rev. Lett.*, vol. 22, pp. 1320–1324, Jun 1969.

[60] M. Maggiore, "Gravitational wave experiments and early universe cosmology," *Phys.Rept.*, vol. 331, pp. 283–367, 2000.

[61] G. M. Harry, "Advanced LIGO: The next generation of gravitational wave detectors," *Class.Quant.Grav.*, vol. 27, p. 084006, 2010.

[62] B. Caron, A. Dominjon, C. Drezen, R. Flaminio, X. Grave, *et al.*, "The Virgo interferometer," *Class.Quant.Grav.*, vol. 14, pp. 1461–1469, 1997.

[63] P. Amaro-Seoane, S. Aoudia, S. Babak, P. Binetruy, E. Berti, *et al.*, "Low-frequency gravitational-wave science with eLISA/NGO," *Class.Quant.Grav.*, vol. 29, p. 124016, 2012.

[64] J. F. Dufaux, A. Bergman, G. N. Felder, L. Kofman, and J.-P. Uzan, "Theory and Numerics of Gravitational Waves from Preheating after Inflation," *Phys.Rev.*, vol. D76, p. 123517, 2007.

[65] D. G. Figueroa, J. Garcia-Bellido, and A. Rajantie, "On the transverse-traceless projection in lattice simulations of gravitational wave production," 2011.

[66] D. G. Figueroa, *Aspects of Reheating*. PhD thesis, Madrid, 2010.

[67] L. B. Bethke, *Exploring the Early Universe with Gravitational Waves*. PhD thesis, Imperial College London, 2014.

[68] G. Rigopoulos and E. Shellard, "The separate universe approach and the evolution of nonlinear superhorizon cosmological perturbations," *Phys.Rev.*, vol. D68, p. 123518, 2003.

[69] C. Cutler and D. E. Holz, "Ultra-high precision cosmology from gravitational waves," *Phys.Rev.*, vol. D80, p. 104009, 2009.

[70] R. D. Sorkin, "Forks in the road, on the way to quantum gravity," *Int.J.Theor.Phys.*, vol. 36, pp. 2759–2781, 1997.